Implementation of an Experimental Platform for Emulation of Grid-Connected Pico-hydro Systems

Paulo Henrique Alves de Araújo

Dissertation Presented to the School of Technology and Management of Polytechnic Institute of Bragança to the Fulfillment of the Requirements for the Master of Science Degree in Industrial Engineering (Electrical Engineering branch), in the scope of double degree with Federal University of Technology - Paraná

Supervised by:
Professor Ph.D. Américo Vicente Teixeira Leite
Professor Ph.D. Ângela Paula Barbosa de Silva Ferreira
Professor Ph.D. Gilson Junior Schiavon

Bragança
2018

Implementation of an Experimental Platform for Emulation of Grid-Connected Pico-hydro Systems

Paulo Henrique Alves de Araújo

Dissertation Presented to the School of Technology and Management of Polytechnic Institute of Bragança to the Fulfillment of the Requirements for the Master of Science Degree in Industrial Engineering (Electrical Engineering branch), in the scope of double degree with Federal University of Technology - Paraná

Supervised by:
Professor Ph.D. Américo Vicente Teixeira Leite
Professor Ph.D. Ângela Paula Barbosa de Silva Ferreira
Professor Ph.D. Gilson Junior Schiavon

Bragança
2018

Dedication

to my parents and my sister,

who have always believed and supported me.

Acknowledgments

I acknowledge and express thanks to both Federal University of Technology - Paraná (UTFPR), Campus Campo Mourão and the Polytechnic Institute of Bragança (IPB) for the opportunity provided and for all the effort made by these two institutions and the people who represent it, that allowed me this study and research opportunity.

I appreciate all the help and patience that my mentors Professor Ph.D. Vicente Leite, Professor Ph.D Ângela Ferreira, and Professor Ph.D Gilson Schiavon had with me during our working in this project.

I would like to acknowledge Eng. Wellington Maidana, Prof. José Batista, Prof. Luis Queijo, Eng. Jorge Paulo and Eng. Abílio Marcelo, for the assistance provided.

I also like to thank my mother Fátima, my father Henrique and my sister Natália, for the support and encouragement during all these years, without them this project would not be possible. My friends who back me up and were with me during this work.

Abstract

Even with technological development, and the increase in the use of renewable energy sources in recent years, 14% of the global population still does not have access to electricity. Pico-hydro systems can be a solution both for lack of grid access and for distributed generation. One of the main challenges for this technology dissemination lies in the fact that the design of the system depends on the characteristics of the place where it will be installed. Thus, a platform that allows the emulation of real conditions in a controllable environment is an interesting option to estimate the system requirements and its production. This work describes the implementation of an experimental platform for emulation and analysis of pico-hydro systems, grid-connected and also stand alone solutions. With this platform, tests were carried out on 4 types of turbines connected to the electric grid. A low head turbine (1,5 to 5 m) propeller type, a Turgo turbine for heads up to 30 m, a pelton turbine for heads up to 90 m and a horizontal water wheel. The tests carried out with the propeller turbine and the water wheel are fundamental for the ongoing projects in the House of Silk and the Castrelos Aquaculture Centre.

Keywords: pico-hydro systems; grid-connection; turbines; renewable energy.

Resumo

Mesmo com o desenvolvimento tecnológico e o aumento na utilização de fontes de energia renováveis nos últimos anos, 14% da população mundial ainda não possui acesso a rede elétrica. Sistemas pico-hídricos podem ser uma solução tanto para falta de acesso a rede, quanto em relação a geração distribuída. Um dos principais desafios para a disseminação dessa tecnologia, está no fato de que o projeto do sistema depende das características do local onde este será instalado. Assim, uma plataforma que possibilite a emulação de condições reais em ambiente controlável é uma opção interessante para estimar os requisitos do sistema e sua produção. Este trabalho descreve a implementação de uma plataforma experimental para a emulação e análise de sistemas pico-hídricos, ligados a rede ou isolados. Com esta plataforma, foram realizadoos ensaios em 4 tipos de turbinas ligadas a rede elétrica. Uma turbina de baixa queda (2 - 5 m) do tipo hélice, uma turbina tugo para quedas até 30 m, uma turbina pelton para quedas até 90 m e uma roda de água horizontal. Os ensaios realizados com a turbina de hélice e a roda de água são fundamentais para os projetos em curso na Casa da Seda e no Centro Aquícola de Castrelos.

Palavras-chave: sistemas pico-hídricos; conexão a rede; turbinas; energias renováveis.

Contents

List of Tables

List of Figures

Acronyms

AC alternate current.

DC direct current.

DG distributed generation.

IPB Polytechnic Institute of Bragança.

LSE Electromechatronic Systems Laboratory.

MPP maximum power point.

MPPT maximum power point tracking.

PM permanent magnet.

PMSG permanent magnet synchronous generator.

PV photovoltaic.

Symbols

H head.

I_{DC} load current.

I_g generator current.

N speed.

PF_g power factor of the generator.

P_{DC} continuous power.

P_{gross} gross power.

P_g power of generator.

P_{net} net power.

Q flow rate.

R^2 coefficient of determination.

V_{DC} DC voltage.

V_{LL} line-to-line voltage.

V_{oc} open circuit voltage.

V_o output voltage.

η overall efficiency.

ρ_{water} density of water.

f_{se} electric frequency.

g gravitational acceleration.

n_m synchronous speed.

n_{noload} no load rotor speed.

n_{rotor} rotor speed.

p number of magnetic poles.

Chapter 1

Introduction

The increasing concern about the use of fossil fuels and their impact on the environment, the need for diversification of the energy matrix, coupled with rising energy demand, have boosted the use of renewable energy sources in the last two decades [1][2].

According to the Energy Access Outlook 2017, from International Energy Agency, 1,1 billion people (14% of global population) do not have access to electricity [3]. Pico-hydro systems can be a solution for the lack of access to the electrical grid in isolated areas in developing countries [4], likewise, it has an untapped potential in distributed generation in developed countries [5].

The estimated electrical yield of 1 kW pico-hydro system, working 70% of the year due to seasonal changes and maintenance, is 6132 kWh/year. As a means of comparison, according to the real data of photovoltaic (PV) units installed at Polytechnic Institute of Bragança (IPB), the annual production is 1466,9 kWh per 1 kWp installed [6]. With the same installed power, the pico-hydro produces more than 4 times the PV production.

There are differences in the installation design for each case, thus, an experimental platform that allows the testing of turbines in real conditions, before the installation, is a very interesting option. Especially for projects in progress, in House of Silk and Castrelos Aquaculture Centre, that will be explained in the course of this dissertation.

1.1 Objectives

This dissertation is focused on the implementation of an experimental emulation platform for grid connected pico-hydro systems, for educational and applied research purposes and specifically for ongoing projects. The grid-connection is made by using photovoltaic inverters, a mature, cheap and widely available technology.

For these purposes the following steps were achieved: the characterization of three pico-hydro turbines; grid-connection tests using generators connected to photovoltaic inverters; emulation of turbines at real conditions, and discussion of these tests.

1.2 Document Structure

This dissertation is composed of five chapters. This first chapter presents an introduction of pico-hydro systems as well as the proposal and framework of this document.

The second chapter presents the state of the art, a theoretical review of hydropower systems, focusing on pico-hydro, the technologies used in these systems (turbines and generators) and the concept of distributed generation.

The third chapter presents the description of the experimental platform and its implementation.

The fourth chapter presents the obtained experimental results and the proper discussion.

Lastly, the fifth chapter presents the conclusion, as well as the suggestion for future works.

Chapter 2

State of The Art

The increasing demand for electricity, as well as the depletion of fossil fuels and their adverse impact on the atmosphere, have led to intensive research in the renewable energy area. Various renewable energy sources have already been explored, including wind, solar and biomass. Small-scale hydropower plants can be an interesting and almost an untapped way to contribute to electrical production from a renewable source. It is cost-effective and environmentally friendly. This kind of electricity generation can be a way to fulfil the lack of electric grid in rural and remote areas, especially in developing countries. In developed countries, with the well-established and stable power grids, the small-scale hydropower can contribute to supply the increasing energy demand. Furthermore, the integration of distributed generation under the microgrids concept, is an innovative solution for electrification of remote regions and for the exploration of renewable energies and self-sustaining systems, while decreasing the stress in electric power transmission.

2.1 Hydroelectricity

About 71% of the Earth's surface is covered by water, less than 1% of this percentage is from fresh water, although the percentage seems to be insignificant, it plays an important part on the world energy matrix. Hydropower provides about 16,4% of the world's electricity from all sources [7].

The Hydropower plants can be classified by the size of installed capacity, i.e., the intended full-load sustained output, as shown in Figure 2.1.

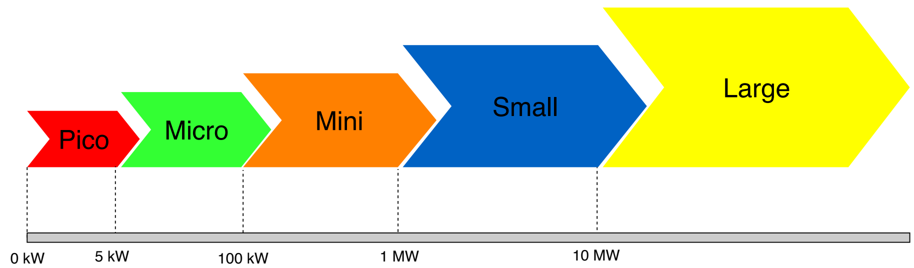

Figure 2.1: Classification of Hydropower. Adapted from [4].

Most of the hydropower available can be categorized as Large Hydro, nevertheless, studies indicate that plants that produce hydropower of more than 1 MW cannot be considered as a renewable energy [8][9]. This is due to the considerable environmental impacts, which generally involves large dams construction, intensive deforestation, greenhouse gas emissions, and also social drawbacks like removing people from their roots [4][9]. Small hydro plants do not suffer from these environmental and social problems, due to its small scale of technology and the insignificant or no storage of water [9].

2.1.1 Power from water

The determination of the power of water flowing in a river or stream requires water flow rate and a drop in high (referred to as a 'head') [10][11]. The power available from falling water can be calculated as follows:

$$P_{gross} = \rho_{water} Q H g \tag{2.1}$$

where P_{gross} is the gross power [W], ρ_{water} is the density of water [kg/m^3], Q is the flow rate [m^3/s], H is the head [m] and g is the gravitational acceleration [m/s^2].

Nonetheless, no power conversion system can deliver as much useful power as it absorbs, there is some power loss in form of noise, friction, heat, and others. Therefore, the net power can be calculated as follows:

$$P_{net} = \eta P_{gross} \tag{2.2}$$

where η is the overall efficiency and P_{net} is the net power [W].

2.2 Pico-hydro generation

Small-scale hydropower generation has been an alternative to fill the lack of reliable electricity, especially in rural and remote areas without access to the grid, where is difficult and expensive to implement conventional transmission lines [4].

Hydro systems that generate electric power up to five kilowatts are denominated pico-hydro [5] and this type of systems is usually run-of-river applications that use very small or no dams or reservoirs [8]. Normally stand-alone, pico-hydro systems usually consist of a turbine driving a generator, and a load controller used to regulate the voltage and frequency [5][12]. Figure 2.2 shows an example of a typical layout of micro-hydro generation.

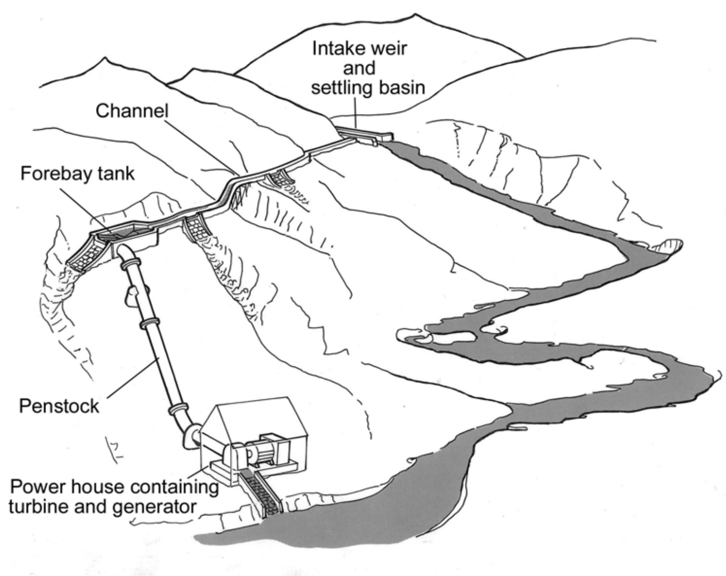

Figure 2.2: Layout of a typical micro-hydro scheme [13].

In the current literature, there has been a growth in the studies of small-scale plants, such as mini, micro, and pico-hydro, being an environmental, cost-effective and efficient solution for renewable energy production [4]. Another important feature in these systems is its ability to be producing electric energy during the whole year around 24 hours a day, presenting high reliability (if properly designed) and low operating costs [14].

Moreover, pico-hydro grid-connection systems are an emergent solution for a large number of applications, such as in small unexplored water courses, domestic water supply systems and wastewater treatment plants. They are still very promising for integration into smart micro-grids. This type of connection has been facilitated using wind and photovoltaic inverters and low speed generators with off-the-shelf low power solutions for wind systems. The wind and photovoltaic inverters, in 5 kW range, are cheap with mature and reliable technology widely available [15][16].

2.2.1 Pico-hydro Systems in Developing Countries

In the reviewed literature, most of the pico-hydro systems were designed to provide electricity to rural communities, especially in developing countries. In these communities, the lack of access to the electrical grid can be mainly explained by geographical isolation, low population density, and the low growth potential of these areas [17]. To extend the existing electrical grid system to those areas, the government authorities have faced many constraints, especially with the high costs of those extensions. Thus, a pico-hydro can be designed and built by local staff and smaller organizations, achieving reduced costs [11]. The electricity produced by pico-hydro turbines is useful to power small loads, such as lamps, televisions, and radios, enabling more comfortable lives for the people in a rural, isolated or hilly areas [4].

Small-scale hydro systems installed in developing countries are generally run-of-river applications. This scheme does not stop the river flow, instead diverts part of the flow into forced channels and pipelines, to run small hydroelectric power stations, being then returned to the catchment [11]. Hydroelectric power stations generally use turbines and generators sized specifically for each application. Some research that corroborates the pico-hydro system concept, presented previously, are described in the following paragraphs.

A case study in Nepal [18] reports the implementation of a pico-hydro system with a minimum output of 4.4 kW, distributed equally to 88 households. The produced electricity allows the population to use lamps and small loads.

Basar *et al* [4] present the efforts of the Ministry of Energy, Green Technology and Water Malaysia to increase the contribution of pico-hydro towards the national electricity supply and sustainable socio-economic development. Furthermore, the government has set a vision, targeting a contribution of 500 MW of small hydro until 2020.

Sopian *et al* [8] from The National University of Malaysia (UKM) present a project to power a factory for processing agriculture products. This pico-hydropower scheme produces 220 V AC and 22 A, resulting in 5 kW of electric power.

Syed *et al* [19] presented a pico-hydropower plant design using the water from irrigation pump used in rural areas in Bangladesh. The solution has presented a way to improve the life quality of a vulnerable community.

South East Asia leads the small-scale hydropower market, with hundreds of thousands of units deployed in the last 15 years in Vietnam, Malaysia, and China. There are many other countries exploring this kind of energy production, including the Philippines, India, Sri Lanka, Laos, Ecuador, Bolivia, Peru and Columbia [20].

2.2.2 Pico-hydro Systems in Developed Countries

In developed countries beyond of rural electrification, the main goals of renewable energy exploration, including pico-hydropower systems, are the environmental concern, the economy, the increasing electricity demand, and distributed generation.

In the literature review it is possible to find several studies being conducted to analyze the possibility of taking advantage of the pressure of public water supply or waste treatment systems as an advantage, to move turbines producing electricity [21][22][23].

Machado [21] proposes the substitution of pressure-relief valves, in water supply systems, to power on microturbines, achieving the control of the pressure along with short-scale electricity production. The study demonstrates through simulations the feasibility of this type of solution.

Another interesting project developed in the city of Boulder, Colorado in the United States, describes that 7% of the electrical consumption of 125,000 residents is provided by 5 turbine-generators installed within its municipal water supply system [22]. The project involved the installation of the turbines coupled to electric generators at points where pressure-relief valves were located, using the water flowing excess pressure to produce electricity.

Since 2016, in the scope of the SilkHouse project, a smart micro-grid, based on renewable energy is being developed, with the aim of making a science dissemination museum "House of Silk", in Bragança, Portugal, into a self-sustaining building in annual average terms. One of the renewable energy sources to be exploited is a pico-hydropower plant. The pico-hydro turbine used in the project is a 1600 W propeller turbine with an estimate energy production of 6,5 MWh/year [24].

In the BIOURB NATUR project sphere, a smart micro-grid based on pico-hydropower generation and photovoltaic generation, is being developed, with the goal to make the Castrelos Aquaculture Centre a self-sustaining building [25].

2.3 Turbines

This section presents the main turbine technologies used in pico-hydropower systems.

Turbines have been used throughout the world to convert available mechanical energy from natural resources like rivers and wind, through various societies and cultures for centuries. Once that water is used as the working fluid, the turbines are categorized as hydraulic turbines or hydro turbines [26]. The turbine's rotating part is called the runner. The runners used in hydroelectric systems have different shapes and sizes, such as vanes, blades, or buckets that rotate about an axis by the action of water [27].

There are two categories of turbines: the positive-displacement and dynamic ones. While the most part of the positive-displacement turbines are devices used for volume flow rate measurement, the dynamic turbines, are used both for volume flow rate measurement and power production [26].

Dynamic turbines can be crudely classified as high, medium or low head machine, as shown in Table 2.1, and regarding its operating principle, they can be grouped into two types: impulse and reaction turbines [11][26].

The selection of the hydro turbine for a plant is based on many aspects, that can include: water head, flow or volume of water available on the site, the turbine efficiency, and cost [28]. The Figure 2.3 presents the relation between the net head and flow ranges of micro-hydro turbines.

Table 2.1: Groups of Impulse and Reaction turbines [11].

	Head Pressure		
Turbine Runner	**High**	**Medium**	**Low**
Impulse	Pelton Turgo Multi-jet Pelton	Crossflow Turgo Multi-jet Pelton	Crossflow
Reaction	-	Francis Pump-as-turbine (PAT)	Propeller Kaplan

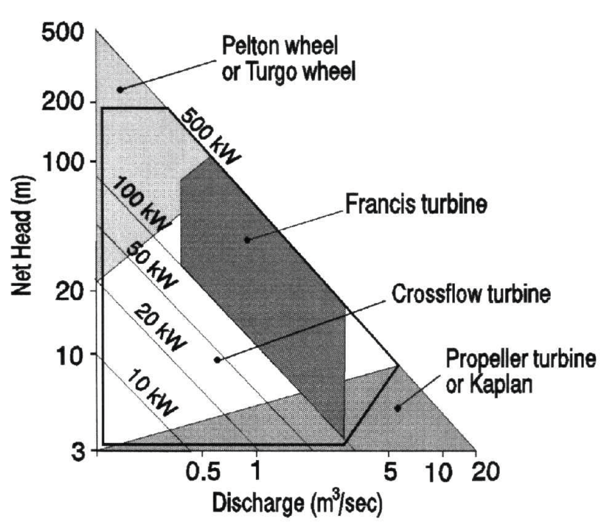

Figure 2.3: Head vs flow ranges of micro-hydro turbines [29].

2.3.1 Impulse Turbines

The impulse turbine uses the kinetic energy of water, in form of a jet (or jets), to drive the runner, that operates in air, and discharges at atmospheric pressure [29][30]. There is no suction on the downside of the turbine. Generally, the impulse turbine operates better with high or medium head, above 10 meters [31]. There are three main types of impulse turbines: Pelton, Cross-flow and Turgo, as shown in Figure 2.4.

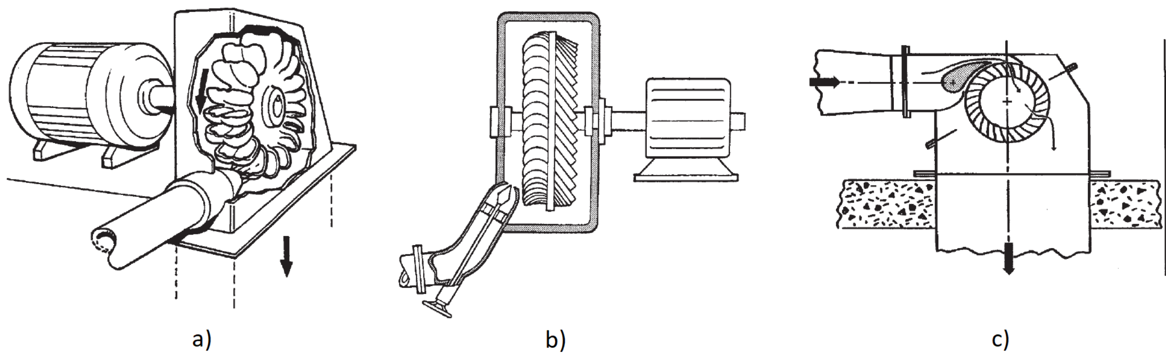

Figure 2.4: a) Pelton turbine. b) Turgo turbine. c) Cross-flow turbine. Adapted from [29].

Pelton Turbine

The Pelton turbine can contain one or multi high-velocity jets of water that hits tangentially a series of split buckets (vanes) [30]. The jet is split in half and each half is turned and deflected in a maximum angle rate of 165°, in order to the returning jet does not interfere with the next bucket [11]. This type of turbines does not require a draft tube, considering its runner is positioned above the maximum tailwater, that permits operation at atmospheric pressure [32]. Pelton turbines are frequently applied in systems with large water heads and low flow rates. Moreover, it has advantages for installations where is present in the water, abrasive matter and for long-penstock where water hammer is critical [27][28][33]. This kind of turbine was invented in 1878 by Lester A. Pelton (1829-1908) and is now named in his honor [26].

In Figure 2.5 is shown the runner of a pico-hydro Pelton turbine, model PLT350 HP from PowerSpout, with output power of 1600 W, available in Electromechatronic

Systems Laboratory (LSE) at IPB. The turbine has been used in the research platform and is described in the next chapter.

Figure 2.5: PLT350 HP runner.

Turgo Turbine

The turgo turbine is analogous to Pelton turbine. However, the buckets have a different shape, they look like the Pelton bucket cut into half [29]. The water stream is applied on one side, at a specific angle, goes across the blade and exits on the other, therefore, the incoming jet and the discharged fluid do not cross each other [28]. The turgo turbine was invented in 1920 by Eric Crewdson of Gilbert Gilkes and Co. Ltd. [30]. The turgo turbine's efficiency depends on many factors, including, nozzle or jet inclination, cup design, and speed ratio [33]. References [34] and [35] define that the jet angle inclination to achieve the peak efficiency is approximately 20°. The main advantage of turgo turbine comparison with a Pelton turbine, is that a larger jet can be applied, resulting in a higher speed, consequently, it can have a small diameter, for an equivalent power [29].

The runner shown in Figure 2.6 is from a pico-hydro turgo turbine, the TRG350 HP from PowerSpout, with an output power of 1600 W. The turbine is available in LSE at IPB, and is described in the next chapter.

Figure 2.6: TRG350 HP runner.

Cross-flow Turbine

The cross-flow turbine, also known as, Bunki-Michell or Ossberger, is another significant impulse turbine. This type of turbine is commonly applied in lower heads and higher flow rates than Pelton and turgo turbines [33]. The cross-flow turbine allows the water flow through the blades twice, first from the outside of the blades to inside, and then from the inside back out [28]. The blades are shaped, such that, at each passage through the runner, the water transfers part of its momentum, consequently, falling with little residual energy [29]. The Banki-Michell turbine is often used in low power range, its efficiency is lower than conventional turbines, such as Pelton, turgo, propeller (Kaplan) and Francis, but, on the other hand, the efficiency remains constant in a wider range of flow rates [21]. A cross-flow turbine runner is shown in Figure 2.7.

Figure 2.7: Cross-flow turbine runner [36].

2.3.2 Reaction Turbines

The reaction turbine generates electricity by the mutual action of moving water and pressure [30]. In reaction turbines, the runner is fully immersed in water and is enclosed in a pressure casing [11]. Compared with impulse turbines, reaction turbines have a better performance in high flow sites with lower heads, and its efficiency is higher at low operating speeds [33].

In reaction turbines, draft tubes are used as the final component of the water passage. It is a pipe that usually increase the area gradually, and connect the outlet of the runner to the tailrace (a channel that carry away the water discharged from the turbine). The draft tube provides the recovery of a portion of kinetic energy into useful pressure, increasing the net head on the turbine [27]. There are two main types of reaction turbines: propeller and Francis as shown in Figure 2.8.

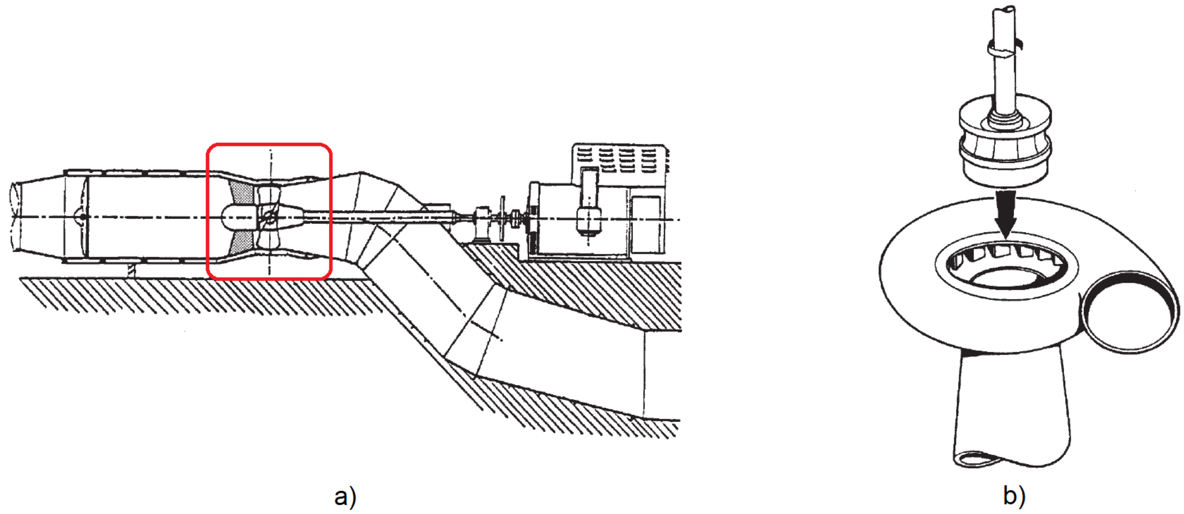

Figure 2.8: a) Tube-type propeller turbine. b) Francis turbine. Adapted from [29].

Propeller (Kaplan) Turbine

The propeller turbine commonly has an axial flow runner containing three to six blades [30]. To achieve a good efficiency, the water needs to be given some swirl before entering the runner. If the design is good, the swirl is absorbed, and the water goes into the draft tube with a little residual angular momentum [29]. A propeller turbine with coordinated adjustable blades is called Kaplan, in honor of its inventor Viktor Kaplan [27]. This adjustment of the blades can considerably increase the efficiency, however, it is costly and may be economically viable only in bigger systems [29]. Propeller turbines are suitable for systems with low water heads [30]. In general, the propeller turbines rotate faster than the Francis and impulse turbines (given the same head and flow conditions). These high speeds imply that reaction turbines can often be directly coupled to an alternator without any speed-increasing drive or gearbox [11].

Figure 2.9 shows the three blades runner of a pico-hydro propeller turbine, model LH400, from PowerSpout, with an output of 1600 W. The turbine is available in LSE at IPB and is described in the following chapter.

Figure 2.9: Propeller turbine runner.

Francis Turbine

The Francis turbine is the most commonly used type at hydropower stations [30]. It is essentially a modified propeller turbine, in which the water flows radially into the runner and emerges axially [29]. The runner of Francis turbines has fixed vanes, usually nine or more [28]. The other important components of a Francis turbine are the scroll case, wicket gates, and draft tubes [21]. This kind of turbine is widely adaptable to different water heads and flow rates [21]. The runner of a Francis mixed-flow turbine used at the Smith Mountain hydroelectric power station in Roanoke is shown in Figure 2.10.

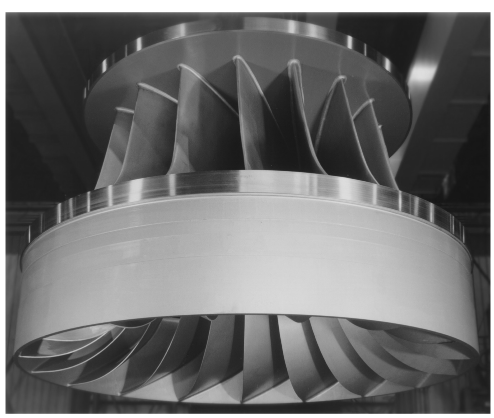

Figure 2.10: Francis turbine runner [26]

.

2.4 Electric Generators

The electric generator is an electric machine that converts mechanical energy from an external source into electrical energy at the output. There are various types of electrical machines available that can be roughly divided into two categories, direct current (DC) machines, and alternate current (AC) machines. The AC machines are subdivided into Synchronous and Induction (or Asynchronous) devices. The selection of the generator for a specific application depends on many aspects such as prime mover speed, required output power, the range of operation (voltage) along with the application (e.g. battery charging or grid connection) [20].

To short-scale applications, the DC generators are usually ruled out, mainly due to the necessary maintenance of brushes and slip rings needed for mechanical commutation [20]. Thus, the AC generators are more suitable for pico-hydropower applications.

2.4.1 Induction Generators

The induction machines or asynchronous machines usually need to draw its excitation power from the supply mains or a capacitor bank to work as generators. When the rotor speed increases above the synchronous speed by an external prime mover, it will operate as an induction generator [37][38]. This type of generator is attractive as it is a reliable, robust and cheap option [20].

For the off-grid operation, capacitors banks are required due to the necessity of reactive power [20], consequently, induction generators are best suited for on-grid applications [39].

There are two types of induction rotors, the wound, and the squirrel cage. Squirrel cage rotors are composed of solid aluminum parallel bars, cast into the slots. The bars are shorted together at each end of the rotor by cast aluminum rings [40]. The wound rotors are three-phase rotor windings, with the phases brought out of the rotor through slip rings and brushes. The wound rotors are expensive and require more maintenance than cage rotors [38].

2.4.2 Synchronous Generators

In synchronous generators, the rotor magnetic field is produced either by applying DC current to the rotor winding to create an electromagnet or designing the rotor as a permanent magnet [38]. The electric frequency produced in a synchronous generator is locked (or synchronized) to the mechanical rate of rotation of the generator. They are related by the following equation:

$$n_m = \frac{120 f_{se}}{p} \tag{2.3}$$

where n_m is the rotating field or synchronous speed [rpm], f_{se} is the electric frequency [Hz] and p is the number of magnetic poles. The equation 2.3 is used to induction generators as well, however, in these generators, the rotor speed exceeds the synchronous speed.

In small-scale hydropower plants, the synchronous generators, that are capable of being operated autonomously, are often used in off-grid applications [39].

Permanent Magnet Synchronous Generator

The permanent magnet (PM) machines have wound stator, and the rotor is provided with a permanent magnet pole system [41]. The separate excitation is done by the PM, resulting in no power lost to excite the rotor, differently of another synchronous or induction machines. Additionally, they do not require slip rings and brushes.

The permanent magnet synchronous generator (PMSG) is commonly used in short-scale hydro and wind systems. The efficiency of PM machines is higher than the other generators, including other synchronous generators due to the self-excitation provided by the PM [42]. In addition to these benefits, the PMSG can operate with high power factor. Nevertheless, the permanent magnet materials required to produce these generators are expensive [41].

There are many topologies of PMSG presented in literature, the most commons being the radial flux permanent magnet (RFPM) and axial flux permanent magnet (AFPM) generators [20]. According to Howey [20] in pico-hydro systems, the PMSG are more attractive than induction generators in terms of cost and performance.

2.5 Distributed Power Generation Systems

In the literature, there is no consensus on the definition of distributed generation (DG). A large number of terms and definitions are used, for example, Anglo-American countries use the term 'embedded generation', North American countries the therm 'dispersed generation', in Europe and parts of Asia, the term 'decentralized generation' is also applied for DG [43].

According to Rujula *et al* [44], the difficulty in defining a distributed generation is in the following items:

- It is, in general, not power or voltage-dependent;
- It can be categorized as renewable and non-renewable;
- Geographical location is not a relevant parameter to distinguish distributed generation from central generation;
- It can be either stand-alone or grid-connected;
- It is connected to the grid either directly, using transformers or power electronics.

Due to large variations in the literature, there are some items that the DG can be defined: purpose, location, power delivery area, technology, environmental impact, mode of operation, ownership, and the penetration of distributed energy [43].

Although, there are some definitions that are generally accepted. According to Guerrero *et al* [45] DG is the electricity production, as near as possible of the consumption site, reliable and good quality electrical power. It is similar to the first electrical systems, in the beginnings of the electric industry, but now incorporating the advantages and benefits of the modern technology [46].

The figure 2.11 illustrates a general structure for a DG system. The input power is transformed into electricity by means of a power conversion unit. The electricity produced can be delivered to the local loads or to the electrical grid.

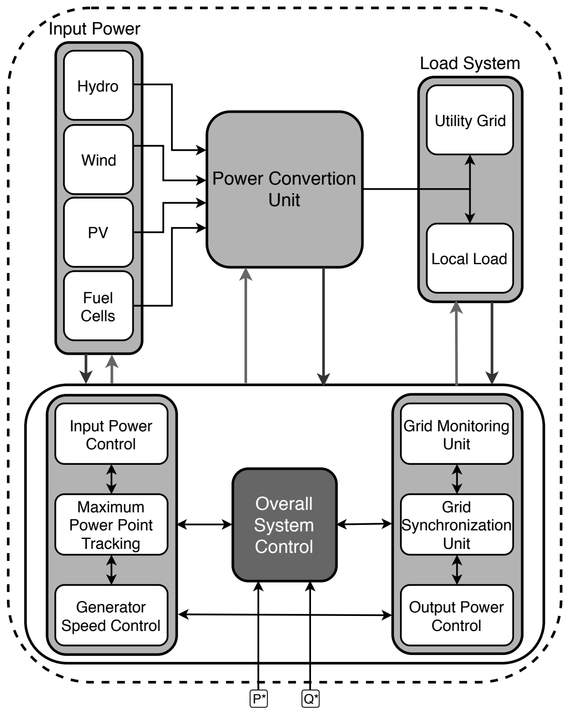

Figure 2.11: General structure for distributed power system having different input power sources. Adapted from [47].

.

The control has an important impact on the distributed generation system and it is divided into two parts. The input-side controller has the main property to extract the maximum power from the input source. The grid-side controller has the task to control the active power generated and the reactive power transferred to the grid, to ensure the high quality of the injected power and grid synchronization [47].

2.5.1 Isolated Systems

The isolated, also known as islanded, stand-alone or off-grid system, is a system that is not connected to the main electrical grid, therefore, must be able to supply electricity by itself at all times. In remote and isolated areas, stand-alone systems can be more cost-effective than extending a power transmission line to the electricity grid [48].

In general, this type of systems has a energy storage, thus allowing the electricity use at times when endogenous resources are not available to produce electricity. The system is generally composed of batteries, charge controllers, power conditioning equipment, safety equipment, meters, and instrumentation, in order to condition and safely transmits the power to the load. Usually, the power conditioning equipment uses a maximum power point tracking (MPPT) algorithm [48].

2.5.2 Grid-connected Systems

The grid-connected or grid-tied system is an electrical generation system that links the generation with the main electrical grid or micro-grid. It allows the injection of the excess electricity produced in the grid, or to draw electricity from the grid, if the production is lower than the demand [49].

This type of system has some requirements, mostly to the power provider, and some equipments are necessary to safely transmit the generated electric energy to the grid. Usually power conditioning units are used for these connections using safety equipments and meters [49]. Each power provider has specific grid-connection requirements.

2.5.3 Hybrid Systems

The hybrid systems are defined as the combination of two or more renewable or non-renewable energy sources [50]. Hybrid systems are capable to operate in both isolated or grid- or microgrid-tied [51].

Energy sources, like wind, solar, hydro, biomass and fuel cells can be integrated to form a hybrid system which is more reliable than single source systems [50]. The utilization of different sources of power and technologies requires more efficient and complex controls than the single source generation.

2.5.4 Case Studies

As an example of distributed hybrid systems, two projects are briefly presented in this section, which are being carried on in the Laboratory of Electro Mechatronic Systems: SilkHouse e BIOURB-NATUR.

SilkHouse Project

The House of Silk is a small science dissemination museum, located in Bragança, in the north-east of Portugal. Within the sphere of SilkHouse Project - Development of a smart microgrid based on renewable energy sources and a monitoring system for the House of Silk-, a renewable energy sources-based micro-grid is being developed, in this case, hydro and photovoltaic. In this project, it will be integrated into the microgrid, a low head propeller type turbine, a horizontal water wheel, and 18 photovoltaic modules, as shown in Figure 2.12. This project aims to make the House of Silk a self-sustaining building in average annual terms. The estimated generation is 15.14 MWh/year, which is very close to the average annual consumption of the museum [24].

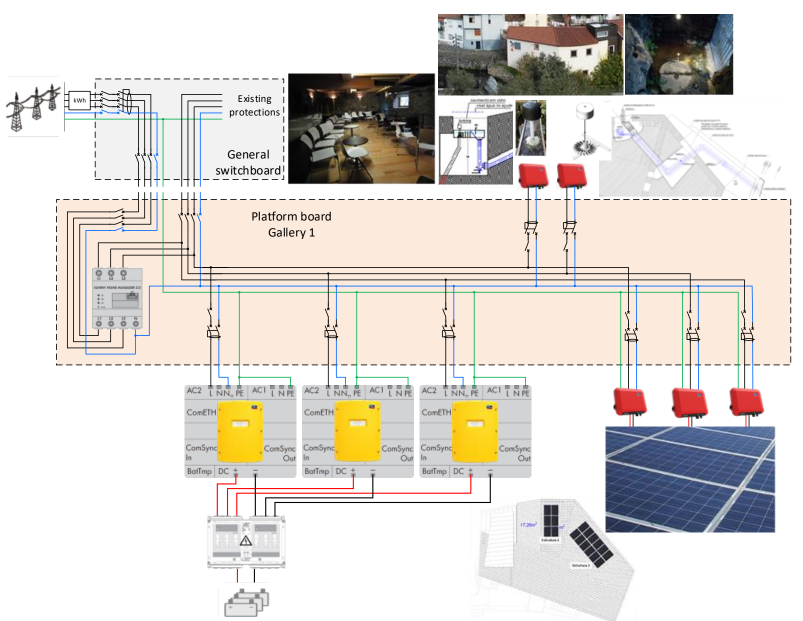

Figure 2.12: House of Silk microgrid scheme, integrating pico-hydro and photovoltaic generation.

BIOURB NATUR

The Castrelos Aquaculture Centre is a building that aims to produce trout for repopulating rivers and watercourses in the region of Bragança, Portugal. Within the scope of the BIOURB NATUR project - Bioconstructive diversity, bioclimatic building, sustainable rehabilitation and its application in natural spaces - an energy solution is being developed to transform the Castrelos Aquaculture Centre into a self-sustaining building on average annual terms. The solution is based on the integration of different renewable source-based power generation, storage, and power management systems into a smart micro-grid as shown in Figure 2.13. The micro-grid is composed of the electric generation of a propeller-type turbine and 32 photovoltaic modules. It has an estimated generation about 15.66 MWh/year [25].

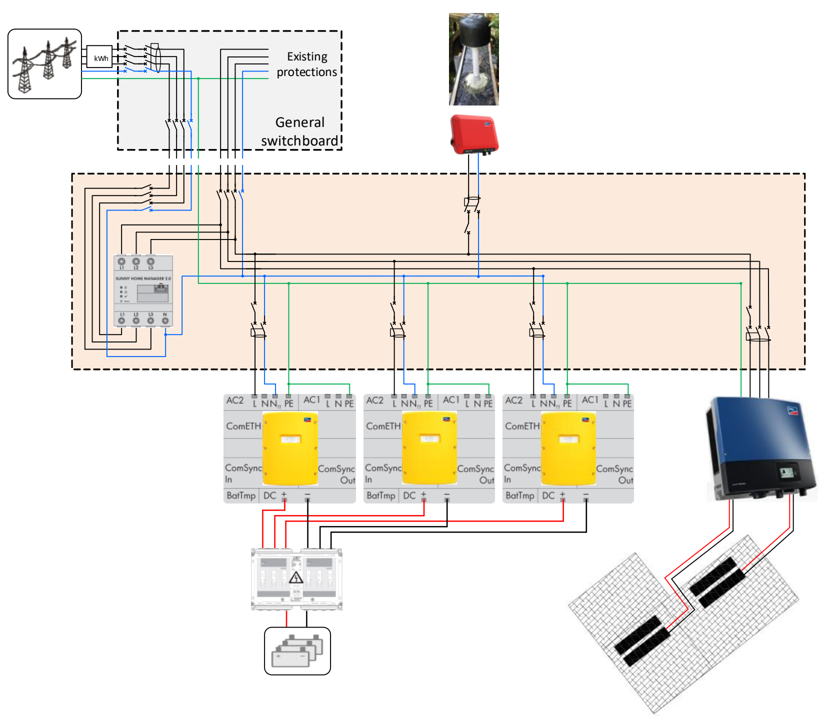

Figure 2.13: Castrelos Aquaculture Centre microgrid scheme, integrating pico-hydro and photovoltaic generation.

Chapter 3

Platform Description

For the implementation of the projects described in subsection 2.5.4, it was necessary to develop an experimental platform to test and evaluate the performance of the pico-hydro turbines and water wheel. The construction of this platform is one of the main objectives of this dissertation, that is described below.

The emulation platform is composed of three distinct and independent systems. The first one is intended for low head turbines, the second one is for heads emulation with medium and high heads turbines and the third one is for a horizontal water wheel. This platform will allow the testing of water turbines up to 1.5 kW, for didactic and applied research purposes and specifically for the ongoing projects, the SilkHouse Project and Catrelos Aquaculture Centre. Figure 3.1 shows the scheme of the platform and distinguishes the three implemented systems.

3.1 Platform Construction

To the proper utilization of a reaction turbine, it is necessary to keep the runner completely submerged in water. In real sites, the water must be extracted from its normal course by an intake and brought to the turbine by a flume or a pipe. In the emulation platform, the flume (water channel) is still necessary to give the right environment to the turbine operation. For this purpose, and for the propeller turbine used in System 1

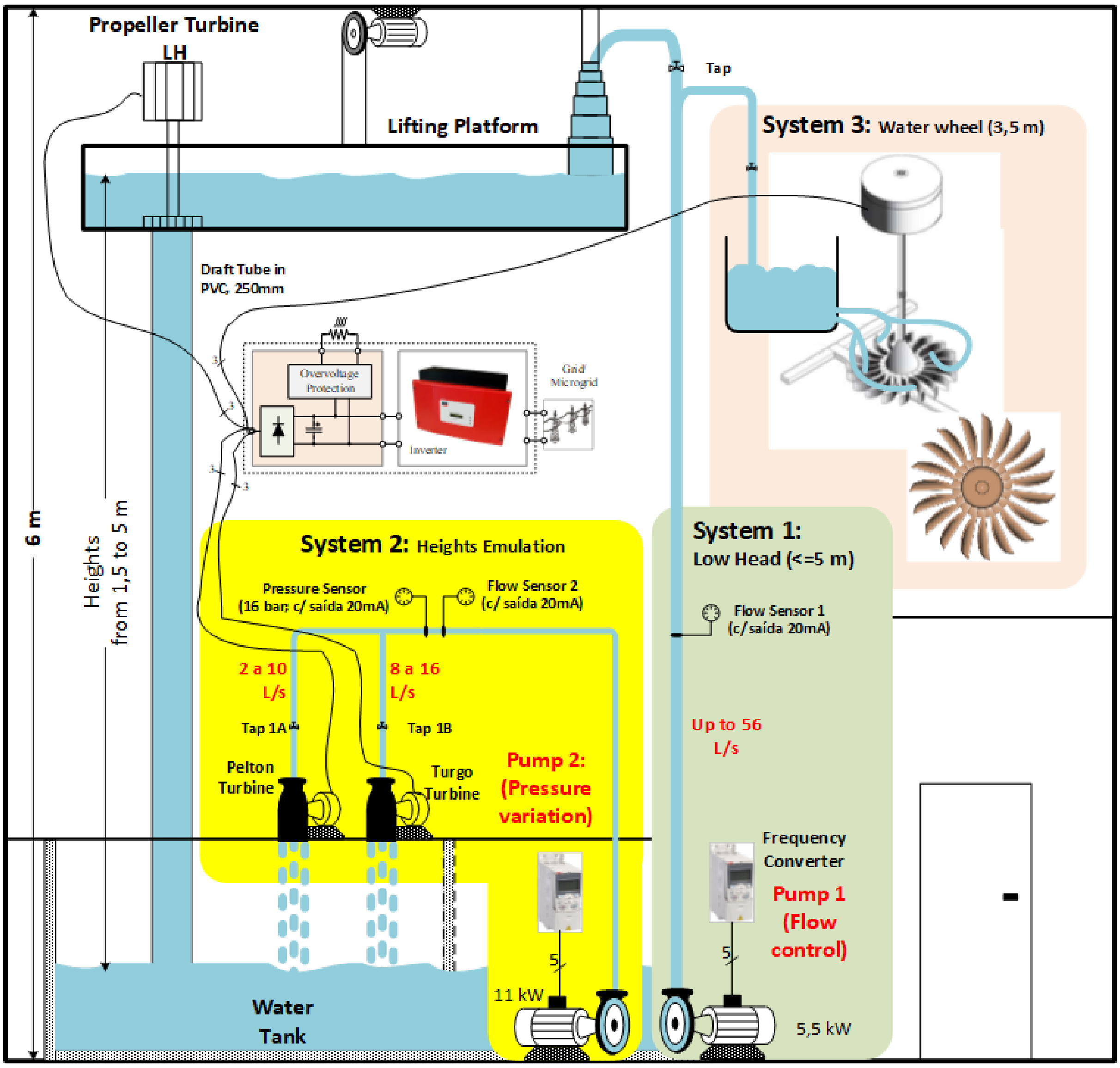

Figure 3.1: Research platform scheme.

(as proposed in Figure 3.1), a stainless-steel flume was constructed, with the support of Mechanical Technology Laboratory, of IPB. The flume was built with dimensions of 0,40 m high, 0,40 m wide, 2,45 m long, and a whirlpool was placed at the end, where the turbine was installed.

The flume first prototype was made of a stainless-steel sheet, folded in two places, as is shown in Figure 3.2. Other stainless-steel sheets were welded to achieve its final design. The flume has been sealed and installed in the Geotechnical Laboratory, at IPB, where the platform is located. The major difficulties encountered in the flume construction were in the sealing, so that there were no leaks, and in the turbulence in which the water was discharged. To avoid spattering and to reduce the turbulence of the water, a tube with fringed plastic was used in the water outlet. It was a temporary solution used to make the tests possible.

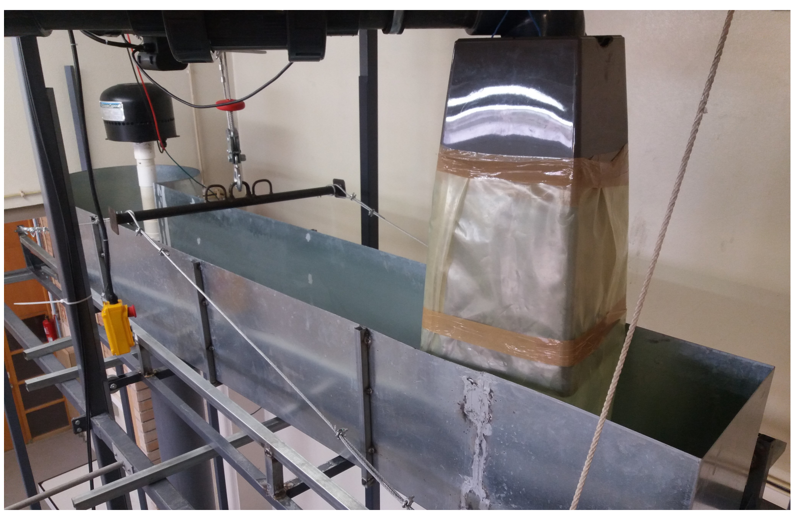

Figure 3.2: Constructed and installed flume for the propeller turbine operation.

To the heads emulation system, it was required the construction of a rigid pipe in iron. The pipe is connected to the pump comprising pressure and flow sensors. There are six outlets in the pipeline, two for the Pelton turbine and four for the turgo turbine. The construction and installation of the electro-mechanical system was performed by a company. The Figure 3.3 shows the pipeline used in System 2 (see Figure 3.1).

Figure 3.3: Pipeline used in the Heads Emulation System

3.2 System 1: Low Head System

The first system is for low-head (up to 5 m) propeller turbines with flow rates up to 56 l/s and it is emulated by means of a water flow sensor and a 5,5 kW pump fed by a frequency converter controlling the water flow.

The turbine used in the first system is a low head, propeller type turbine LH400 from PowerSpout, coupled to a 3-phase permanent magnet synchronous generator (PMSG), 60R110-4S3P-S-HP, from EcoInnovation, with 1600 W of maximum output power. The generator coded as 60R110-4S3P-S-HP is the representation of 36-pole stator, with 0,6 mm copper wire that, and 110 turns per tooth. R code stands for rewound machine. Each phase has 12 coils, 4 coils in series and 3 coils in parallel, and in star connection. The 60R110-4S3P-S-HP is shown in Figure 3.4. The generator has a relation between open circuit voltage (DC voltage of the three-phase rectified output unloaded) and speed V/rpm = 0,211.

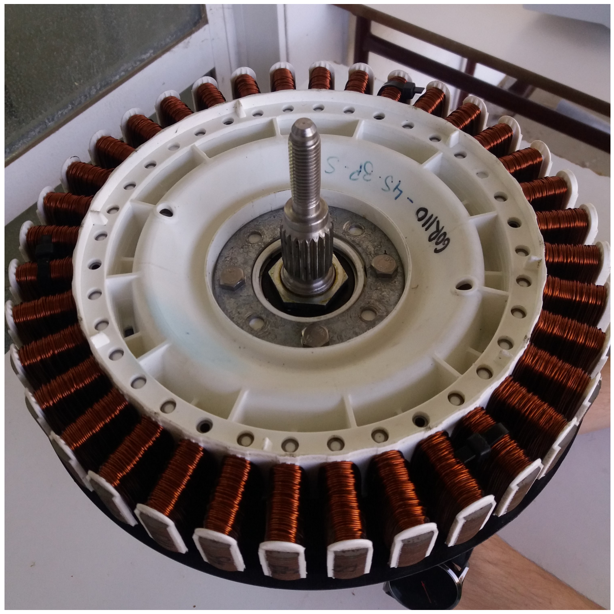

Figure 3.4: 60R110-4S3P-S-HP generator

The technical specifications of LH400 turbine are presented in Table 3.1. The relation between power and head of the LH400 is shown in Figure 3.5, and the relation between flow and head is shown in Figure 3.6, the data used to make the graphs presented in Figure 3.5 and Figure 3.6 were taken from the table flow calculations and generation options of the LH400 turbine installation manual [52].

Table 3.1: LH400 specifications.

Static head range	1 to 5 m
Maximum flow	55 l/s
Minimum flow	25 l/s
Maximum power	1600 W
Maximum current rating	32 A

The estimated values of operation, at maximum flow and maximum head are: output voltage (in load), $V_o = 275$ V, the rotor speed $n_{rotor} = 1500$ rpm. In these conditions, the turbine achieves an output power of 1462 W. The open circuit voltage, $V_{oc} = 487$ V and the no load speed rotor is $n_{noload} = 2308$ rpm.

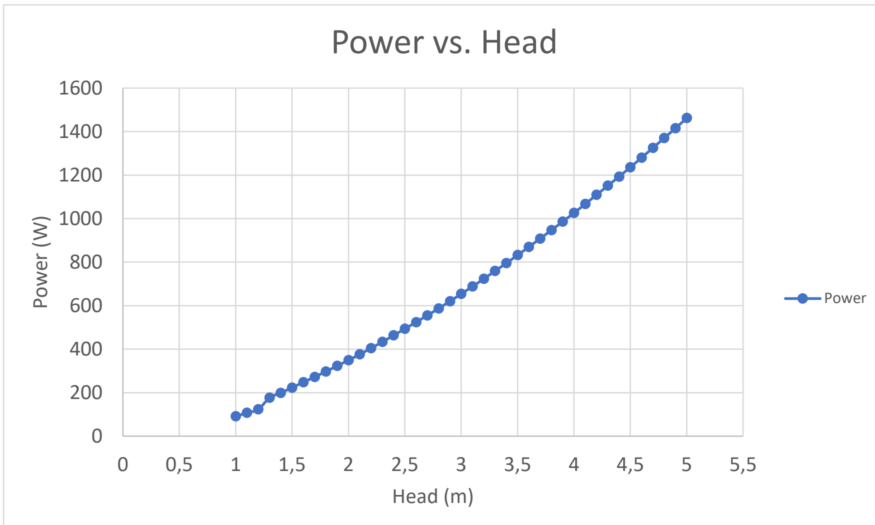

Figure 3.5: LH400 relation power vs. head.

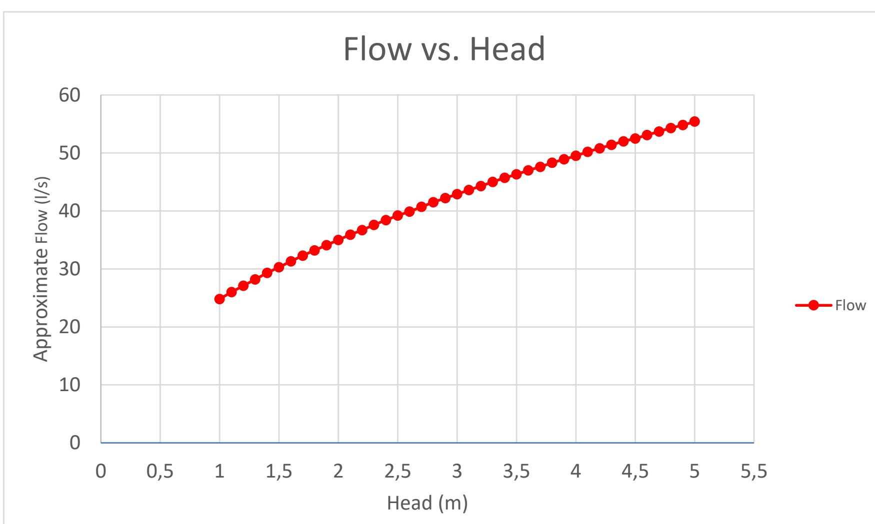

Figure 3.6: LH400 relation flow vs. head.

To acquire flow data it was necessary the use of a flow rate sensor. It was used a VFI

12–240 DN 100 model, from Grundfos. It is a Vortex based sensor, with measuring range between 12 m^3/h and 240 m^3/h and resolution 0,30 m^3/h. The electric data of the sensor is described in Table 3.2.

Table 3.2: VFI 12-240 DN100 specifications [53].

Electrical data	
Power supply	12.5 - 30 VDC (± 5%)
Output signal (-cut off)	4-20 mA (21 mA)
Response time	<1 s
Power consumption	Max. 660 mW
Load impedance	Max 600 Ω at 24 VDC

According to the datasheet, the sensor VFI 12–240 DN 100 output signal has a behavior as shown in Figure 3.7. An output of 4 mA represents the minimum flow measured, 12 m^3/h (approximately. 3.33 l/s), the flow signal is linear and an output of 20 mA represents 240 m^3/h (approximately 67 l/s).

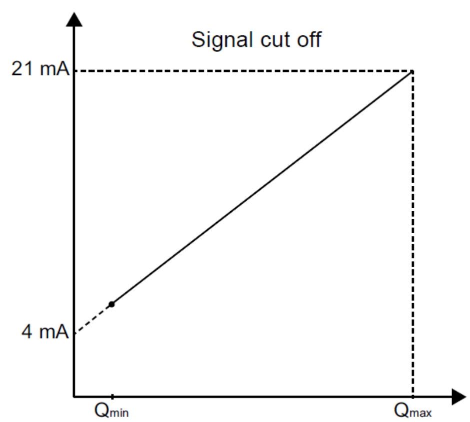

Figure 3.7: Flow sensor output signal [53].

To emulate the right environment for the turbine utilization it is used a single-stage centrifugal pump, model CronoBloc-BL 125/185-5,5/4 from Wilo. The pump standard operating pressure is 1,3 MPa and the maximum ambient temperature is 40°C. The pump motor specifications are described in Table 3.3.

The relation between the manometric head and the flow of CronoBloc-BL 125/185 - 5,5/4 is shown in Figure 3.8. From this figure, and for a water flow of 200 m^3/h

(approximately 56 l/s), the head should be higher than 4 m and less than 8 m.

Table 3.3: CronoBloc-BL 125/185 - 5,5/4 specifications [54].

Motor/electronics	
Mains connection	3∼400 V, 50 Hz
Motor efficiency level	IE2
Rated current (approx.)	11,3 A
Efficiency η_m	0,88
Power factor $cos\varphi$	0,78
Rated power P_2	5,5 kW
Maximum power consumption P_1	6,2 kW
Rated speed n	1450 rpm

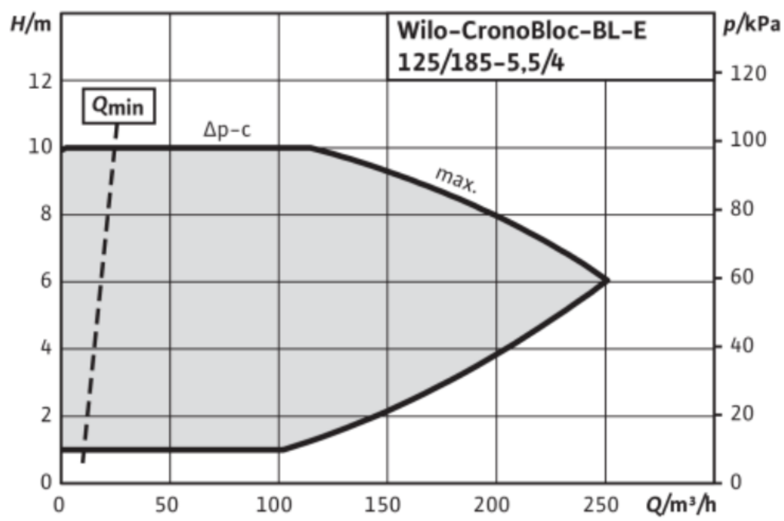

Figure 3.8: Manometric head vs flow of CronoBloc-BL 125/185 - 5,5/4 pump [54].

The frequency converter used to control the pump is the three-phase model ACS355-03E-12A5-4+J404, from ABB, with the specifications described in Table 3.4. The frequency converter ACS355 controls the pump in frequency (Hz), using the macro Standard ABB, the flow sensor output is connected to the ACS355 at the analogic input 1 (AI2) in the pin 5 and is supplied by 24 V_{DC} from the pin 9. The output signal is in current (4-20 mA). The main components used in the system 1 are shown in Figure 3.9.

Table 3.4: ACS355-03E-12A5-4+J404 specifications.

Electric data	
Rated Power (P_N)	5,5 kW
Input voltage (U_1)	3∼400 V/480 V
Input current (I_1)	19 A/16 A
Input frequency (f_1)	48...63 Hz
Output voltage (U_2)	3∼0... U_1 V
Output current (I_2)	12,5 A (150% 1/10 min)
Output frequency (f)	0...599 Hz

Figure 3.9: Low Head Emulation System main components. a) LH400 turbine. b)VFI 12-240 DN100 water flow sensor. c) CronoBloc-BL 125/185-5,5/4 water pump. d)ACS355-03E-12A5-4+J404 frequency converter.

3.3 System 2: Heads Emulation System

The second system is designed for medium and high heads and lower water flows. In this case, a turgo type turbine (up to 30 m) and a Pelton turbine (up to 130 m). The emulation system is achieved using a 11 kW high pressure water pump fed by a frequency converter for water pressure, using a pressure sensor. Additionally, a water flow sensor is also available. The head is emulated by means of the pressure set point.

The Pelton turbine used in the platform is a two jets PLT350 HP, from PowerSpout, coupled to a three-phase PMSG, 60R120-6S2P-S-HP, from EcoInnovation with 1600 W as maximum output power, similar to the generator shown in Figure 3.4. The generator coded as 60R120-6S2P-S-HP is the representation of 36-pole stator, with 0,6 mm copper wire that has 120 turns per tooth. R code stands for rewound machine. Each phase has 12 coils, 6 coils in series and 2 in parallel and star connection. The PLT250 HP turbine's generator has a relation between open circuit voltage (DC voltage of the three-phase rectified output unloaded) and speed V/rpm = 0,345.

The technical specifications of PLT350 HP are shown in Table 3.5.

Table 3.5: PLT350 Hp specifications.

Head range	3 to 130 m
Maximum flow	8-10 l/s
Minimum flow	0,05 l/s (at maximum head)
Maximum power	1600 W
Maximum current rating	32 A

The turgo turbine used in the platform is a 4 jet TRG350 HP, from PowerSpout, coupled to a three-phase PMSG 60R90-6S2P-S-HP, from EcoInnovation with 1600 W as maximum output power, also similar to the generator shown in Figure 3.4. The code 60R90-6S2P-S-Hp represents 36-pole stator, with 0,6 mm copper wire that has 90 turns per finger tooth. R code stands for rewound machine. Each phase has 12 coils, 6 coils in series and 2 in parallel. The generator has a star connection. The technical specifications of the TRG350 HP is described in Table 3.6 and the relation between open circuit voltage (DC voltage of the three-phase rectified output unloaded) and speed V/rpm = 0,259.

Table 3.6: TRG350 HP specifications.

Head range	2 to 30 m
Maximum flow	16 l/s
Minimum flow	8 l/s
Maximum power	1600 W
Maximum current rating	32 A

In order to measure the water pressure, to the head emulation for System 2, it was necessary the utilization of a pressure sensor. It was used an analogical pressure transmitter model XMLG016D21, from Schneider Electric. This sensor has a measuring range between 0 and 16 bar, the destructive pressure is 40 bar and the XMLG016D21 sensor specifications are described in Table 3.7.

Table 3.7: XMLG016D21 specifications [55].

Rated supply voltage	12 V DC, voltage limits: 8...33 V 24 V DC, voltage limits: 8...33 V
Analogue output function	0...20 mA, 2 wire
Current consumption	<20 mA
Response time on output	<2 sec

According to XMLG016D21 datasheet [55], the behavior of its output signal is shown in Figure 3.10. 4 mA represents 0 bar, and it grows linearly until 20 mA, that represents 16 bar (1,6 MPa).

In addition to the use of the pressure sensor, and to have a better control in the input of the turbines, it is used a flow sensor. The flow sensor used is model VFI 3.2-64 DN 50, from Grundfos. It is also a Vortex based sensor, with measuring range between 3,2 and 64 m^3/h and resolution 0,08 m^3/h. The electric data of the sensor is described in Table 3.8. The output signal of the VFI 3.2-64 DN 50 also behaves as the Figure 3.7.

To emulate the head in the system, it was necessary to pressurize the water. For this purpose it was used a high pressure multistage centrifugal pump, model Helix V 3604-1/16/E/KS, from Wilo, in vertical design. The maximum operating pressure of this pump is 16 bar and the maximum ambient temperature is 40°C. The pump motor specifications are described in Table 3.9.

The pump curve of manometric head vs flow is shown in Figure 3.11. Until 100 m, the Helix V 3604-1/16/E/KS can pump about 55 m^3/h (approximately 15 l/s).

The frequency converter used in the system 2 is an ACS355-03E-31A0-4+J400, from ABB, with the specifications described in Table 3.10. The 15 kW ACS355 controls the Helix pump in frequency (Hz), using the Standard ABB macro, the pressure sensor is

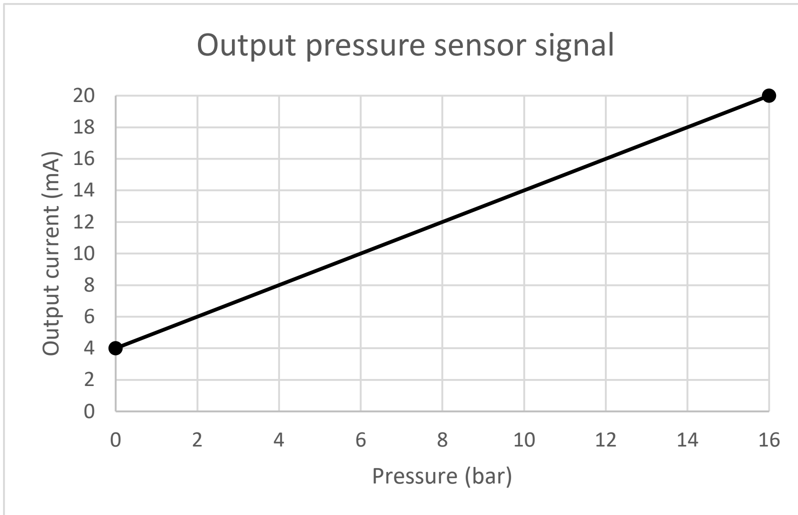

Figure 3.10: XMLG016D21 output signal.

Table 3.8: VFI 3,2-64 DN50 specifications [53].

Electrical data	
Power supply	12.5 - 30 VDC (± 5%)
Output signal (-cut off)	4-20 mA (21 mA)
Response time	<1 s
Power consumption	Max. 660 mW
Load impedance	Max 600 Ω at 24 VDC

supplied by 24 VDC, connected in pin 9, the output signal of the pressure sensor is connected in the analog input 1 (AI1), in pin 2. The flow sensor is supplied by 24 VDC also connected in pin 9, and the output signal of the flow sensor is connected to the analog input 2 (AI2), in pin 5. The output signals of the sensors are in current, both in range of 4...20 mA. The main components used in the system 2 are shown in the Figure 3.12.

Table 3.9: Helix V 3604-1/16/E/KS specifications [56].

Motor/electronics	
Mains connection	3∼400 V, 50 Hz
Motor efficiency level	IE2
Rated current (approx.)	19 A
Efficiency η_m	0,88
Power factor $cos\varphi$	0,78
Rated power P_2	11 kW
Power consumption P_1	12,07 kW

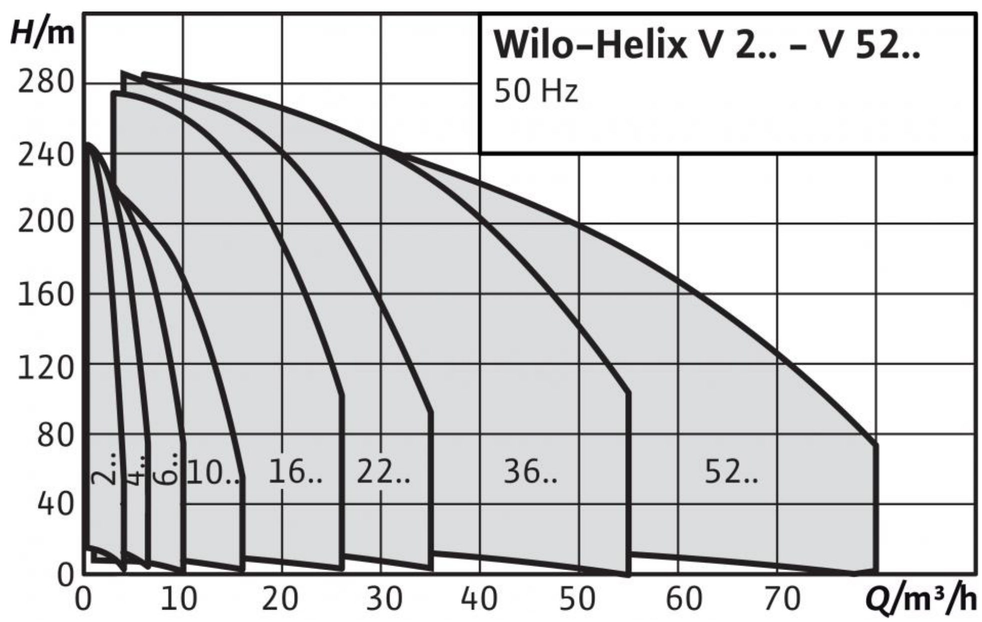

Figure 3.11: Manometric head vs flow of Helix V 3604-1/16/E/KS pump [56].

Table 3.10: ACS355-03E-31A0-4+J400 specifications.

Electric data	
Rated power (PN)	15 kW
Input voltage (U1)	3∼400 V/480 V
Input current (I1)	52 A/43 A
Input frequency (f1)	48...63 Hz
Output voltage (U2)	3∼0...U1 V
Output current (I2)	31 A (150% 1/10 min)
Output frequency (f2)	0...599 Hz

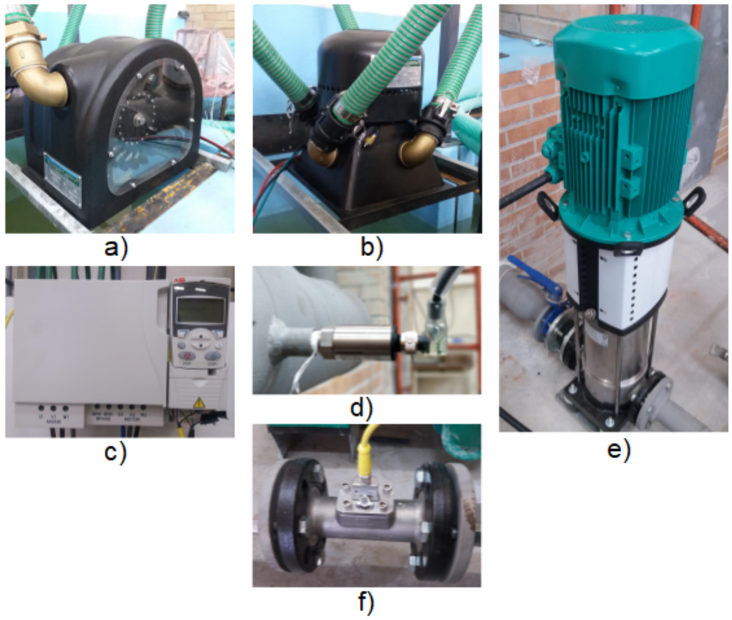

Figure 3.12: Heads Emulation System. a) PLT350 HP turbine. b)TRG350 HP turbine. c) ACS355-03E-31A0-4+J400 frequency converter. d) XMLG016D21 pressure sensor. e) Helix V 3604-1/16/E/KS high pressure water pump. f) VFI 3.2-64 DN50 flow sensor.

3.4 System 3: Water Wheel System

The third system is composed of a horizontal water wheel coupled to a micro wind generator of 300 W and 300 rpm. The water wheel has 36 paddles and 1,2 m diameter. The system also contains a water storage with 1 m^3 of capacity and 4 tubes to the attack jets. The prototyping of the water wheel is described by Dalmarco *et al* [57]. This system share the same area of the other two systems. The system is shown in the Figure 3.13.

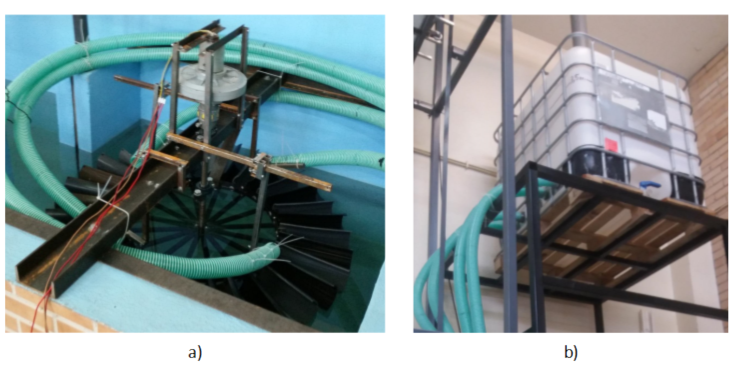

Figure 3.13: a) Water wheel. b) Water storage.

3.5 Grid Connection

The grid connection is made through PV inverters, in an innovative and emergent solution to connect hydro turbines to the grid, as described in [5][15][16]. A PV inverter is a DC-AC converter, that converts the direct current from the PV modules into alternate current that can be tied to an electric grid, microgrid or to off-grid loads. They are a mature and wide available technology, and cheaper than the specifically designed converters for hydro applications. Usually the PV inverters uses maximum power point tracking (MPPT) algorithm and anti-island protection. In the platform, three models of PV inverters were tested to the grid-connection, the three models are single-phase transformerless inverters.

Sunny Boy 1.5-1VL-40, from SMA, is an inverter for small PV systems, with a wide input voltage range from 80 V to 600 V. The inverter has MPPT algorithm and some protective devices installed, such as DC side disconnection point, ground fault and grid monitoring, DC reverse polarity protection and AC short circuit protection [58]. The technical data available of SB1.5 is described in the Table 3.11. The Sunny Boy 1.5-1VL-40 is shown in Figure 3.14a.

Table 3.11: Sunny boy 1.5 technical specifications [58].

Input (DC)	
Max. PV array power	3000 Wp
Max. input voltage	600 V
MPP voltage range	160 V to 500 V
Rated onput voltage	360 V
Min. input voltage/initial input voltage	50 V/ 80 V
Max. input current per string	10 A
Max. short-circuit current per string	18 A
Output (AC)	
Rated power (at 230 V, 50 Hz)	1500 W
Max. apparent AC power	1500 VA
Nominal AC voltage	220 V/230 V/ 240 V
Nominal AC voltage range	180 V to 280 V
AC grid frequency / range	50 Hz, 60 Hz/-5 Hz to + 5 Hz
Rated grid frequency / rated grid voltage	50 Hz /230 V
Max. output current	7 A
Power factor at rated power	1

The second model of PV inverter used in grid-connection of the hydro turbines, is the

Omniksol-2k-TL2, from Omnik New Energy. As protection this type of inverter has, DC insulation monitoring, residual current monitoring unit and grid monitoring with anti-islanding. The technical specifications are described in Table 3.12. The Omniksol-2k-TL2 is shown in Figure 3.14b.

Table 3.12: Omniksol-2k-TL2 technical specifications [59].

Input (DC)	
Max. PV power	2300 W
Max. DC voltage	500 V
Nominal DC voltage	360
Operating MPPT voltage range	120 V - 450 V
Max. input current	18 A
Output (AC)	
Max. AC output power	2200 W
Nominal AC output power	2000 W
Max. output current	11 A
Nominal grid voltage	220 V - 230 V - 240 V
Nominal grid frequency	50/60 Hz
Power factor (cos φ)	0.9 capacitive. . . 0.9 inductive
AC connection	single-phase

The third model of PV inverters used in the plaftform is the Sunny Boy 2100TL inverter, from SMA. The inverter has MPPT algorithm and some protective devices installed, such as DC reverse polarity protection, DC load-disconnecting switch ESS, AC short circuit tolerance, ground fault and grid monitoring. The technical specifications of SB 2100TL is described in Table 3.13. The Sunny Boy 2100TL is shown in Figure 3.14c.

Table 3.13: Sunny boy 2100TL technical specifications [60].

Input (DC)	
Max. DC input power	2200 W
Max. DC voltage	600 V
PV voltage range, MPPT (at rated powe)	125 V - 480 V
Max. input current	12 A
Output (AC)	
Nominal AC output power	1950 W
Max. AC output power	2100 W
Max. output current	11 A
Nominal AC voltage / range	220 V - 240 V / 180 V - 260 V
AC grid frequency (self-adjusting) / range	50 Hz / ±4,5 Hz
Power factor (cos φ)	1
AC connection	single-phase

a) b) c)

Figure 3.14: a) Sunny Boy 1.5-1VL-40. b) Omniksol-2k-TL2. c) Sunny Boy 2100TL

3.6 Over-voltage Protection Circuit

To connect hydro turbines into the grid, by using PV inverters, it is necessary the utilization of an over-voltage protection device. The photovoltaic modules do not present over-voltage characteristics, nevertheless, hydro turbines can reach voltages in open circuit up to 3 times higher than in full operation.

The protection circuit used in the grid-connection of the turbines in the experimental platform was a 3-phase AC input power clamp, model PC AC4 350/400 from PowerSpout, shown in Figure 3.15.

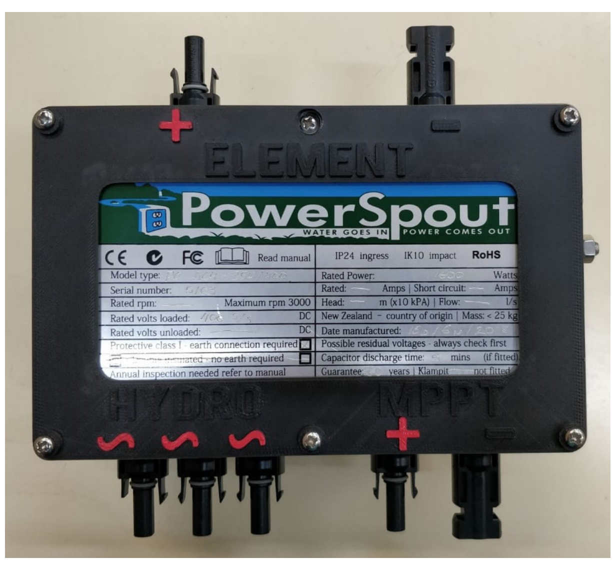

Figure 3.15: PC AC4 350/400.

The power clamp is an external device, connected to the output of the turbine's generator and rectifies its output. Also limits the maximum output voltage of hydro turbines, to protect sensitive equipment such as MPPT, grid-tie inverters or charge controllers. It uses PWM to dissipate the power to heat in a power resistor. Furthermore, it also has a fail-safe crowbar that short-circuits the turbine's entire output current. The specifications of the power clamp is described in Table 3.14.

Table 3.14: PC AC4 350/400 specifications

Model Type	PC AC4-350/400
Rated volts loaded	400 V DC
Rated power	1600 W
Capacitor discharge time	5 min (if fitted)
Ingress protection (IP) rating	IP24
Impact protection (IK) rating	IK10

Chapter 4

Experimental Results and Discussion

This chapter presents the results and proper discussion of the generator characterization, the grid-connection tests in laboratory and the platform real conditions tests.

4.1 Generator Characterization

The permanent magnet synchronous generator (PMSG) characterization is a series of tests with the generator to obtain certain parameters and analyze its behavior, being the procedures described in the following paragraphs. There are two types of tests for the PMSG characterization, no-load tests, and load tests (constant load and variable load). The generator used in these tests was the 60R110-4S3P-S-HP, used in the LH400 turbine.

4.1.1 No Load Test

The setup used in the no-load test is shown in Figure 4.1. It was used a 3-phase induction motor, model 3∼LSMV100L, from Leroy Somer, connected in star and fed by a 3kW frequency converter. In this condition, the motor has 1430 rpm of rated speed, 0,84 cos φ, 400 V, 6,3 A of rated current. The PMSG was directly coupled to the motor and its 3-phase voltages were rectified and connected to a capacitor bank with the equivalent capacitance of 1000 μF. No load was aplied on the generator shaft. For this application, the motor was controlled by the ABB ACS 355-03E-07A3-4 frequency converter. The macro used for this test was the ABB Standard, the speed was chosen as the control variable.

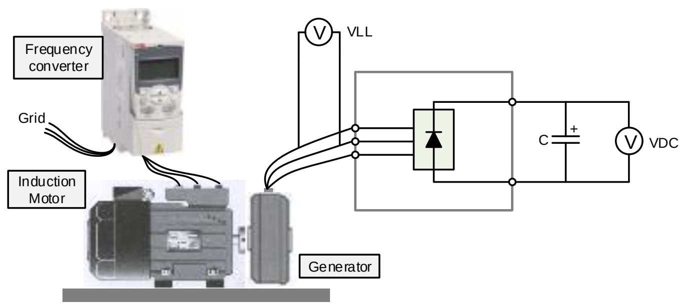

Figure 4.1: No load test setup.

In this test, the line-to-line voltage (V_{LL}) of the generator and the DC voltage (V_{DC}) at the rectifier output were recorded. The V_{LL} was measured with the FLUKE 434 Power Quality Analyzer and the V_{DC} was measured with the FLUKE 85 III True RMS Multimeter. The test was done by varying the motor-generator speed (N) up to the motor rated speed. The test step was 100 rpm. The measured values are described in Table 4.1.

Table 4.1: No-load 60R110-4S3P-S-HP generator test.

N **[rpm]**	V_{LL} **[Vrms]**	V_{DC} **[V]**
0	0	0
100	16,1	22,4
200	31,8	43,5
300	46,7	65,2
400	62,0	86,7
500	77,2	108,2
600	92,4	129,7
700	107,5	151,0
800	122,6	172,4
900	137,7	193,6
1000	152,9	214,8
1100	168,1	236,1
1200	183,1	257,0
1300	198,8	278,0
1400	213,3	299,1
1500	228,2	320,2

The speed-voltage (V_{LL} and V_{DC}) graphs obtained from the no-load test are shown in Figure 4.2. When the speed is increased, the voltages increase proportionally, with coefficient of determination (R^2) equals 1. At 1500 rpm, the V_{DC} voltage is 320,2, with a V/rpm ratio of 0,213, very close to the 0,211-ratio reported by the manufacturer, as described in Section 3.2. Thus, as expected, the output voltage (DC and AC) is proportional to the speed.

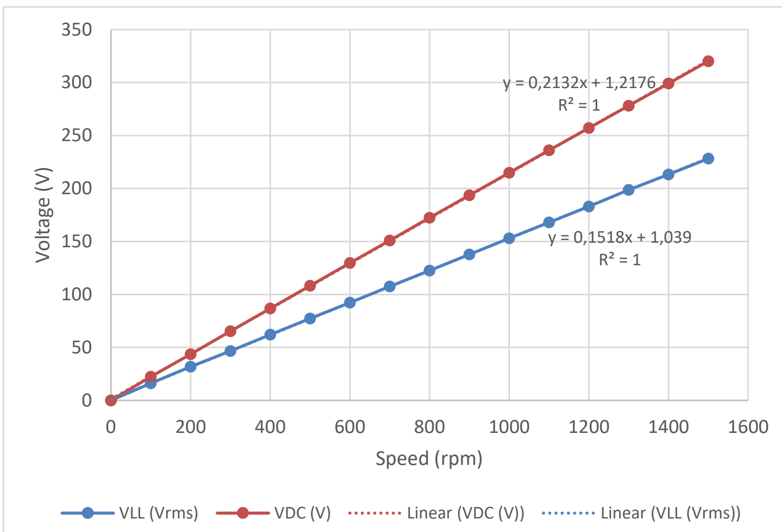

Figure 4.2: No load test with 60R110-4S3P-S-HP generator.

4.1.2 Rated Load Test

The rated load test was done by applying a load (power resistor) at the DC output. The load resistance value was calculated by dividing the square of the rated output voltage V_o by the rated output power P, described in Section 3.2, as follows:

$$R = \frac{V_o^2}{P} = \frac{275^2}{1462} = 51,72\ \Omega \tag{4.1}$$

The setup used in the nominal load test is shown in Figure 4.3.

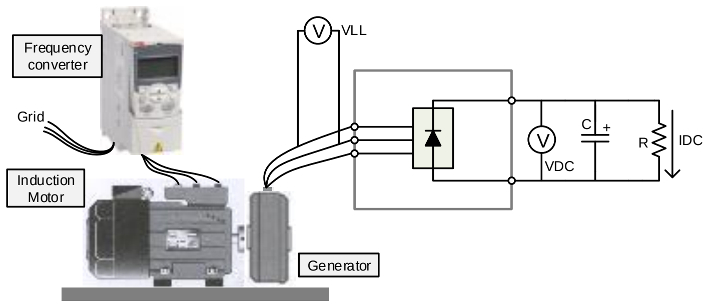

Figure 4.3: Rated load test setup.

The test started with rated speed. Thus, the speed was decreased, and the values are presented in Table 4.2. The measurement of the line voltage (V_{LL}), the generator current (I_g), the power factor of the generator (PF_g), the power of generator (P_g) were measured with FLUKE 434 Power Quality Analyzer. The DC voltage (V_{DC}) measurement was made with the FLUKE 85 III True RMS Multimeter. The load current (I_{DC}) was measured with the TES 2732 Multimeter. This test was performed between 1500 rpm and 500 rpm, in a 100 rpm step.

Table 4.2: Rated load 60R110-S3P-S-HP generator test

N **[rpm]**	V_{LL} **[Vrms]**	$\mathbf{I}_g$ **[A]**	PF_g	$\mathbf{P}_g$ **[W]**	I_{DC} **[A]**	V_{DC} **[V]**	P_{DC} **[W]**
1500	198,5	3,5	0,95	1160	4,74	243,9	1156,09
1400	187	3,3	0,95	1030	4,48	229,5	1028,16
1300	175,3	3,1	0,95	900	4,19	214,8	900,01
1200	163,2	2,9	0,94	780	3,9	199,8	779,22
1100	150,9	2,7	0,94	660	3,6	184,4	663,84
1000	138,2	2,5	0,93	560	3,29	168,8	555,35
900	125,5	2,3	0,93	460	2,99	153,3	458,37
800	112,7	2,1	0,93	370	2,69	138,3	372,03
700	99,5	1,8	0,93	290	2,39	122,8	293,49
600	86,3	1,6	0,93	220	2,08	106,9	222,35
500	72,6	1,4	0,93	160	1,75	90,5	158,38

At 1500 rpm, the generator dissipates 1156 W of power in the power resistor. The relation between the voltages (V_{LL} and V_{DC}) and the load current (I_{DC}) is shown in Figure 4.4. As expected, the relation continues practically linear, both with coefficient of determination (R^2) close to 1.

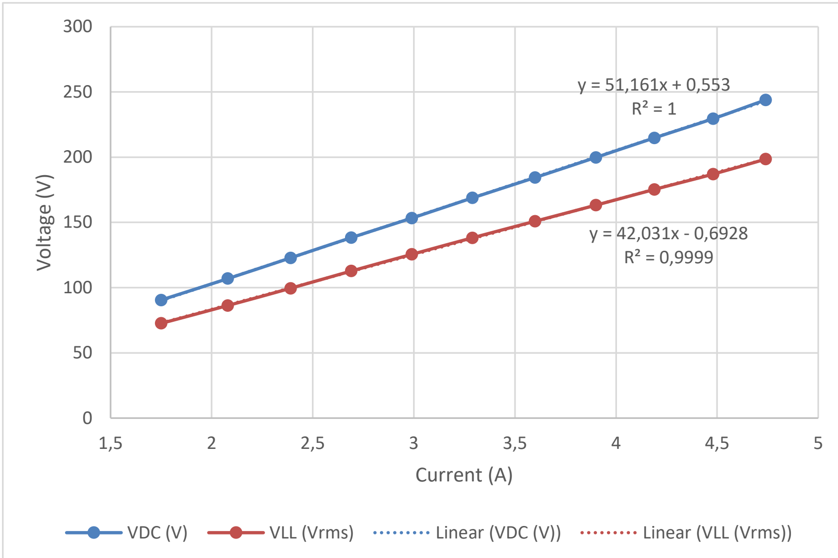

Figure 4.4: 60R110-4S3P-S-HP generator rated load test: I_{DC} vs V_{LL} and V_{DC}.

The relation between the voltages (V_{LL} and V_{DC}) and speed (N) is shown in Figure 4.5. As expected, the relation are practically linear with both coefficient of determination (R^2) close to 1.

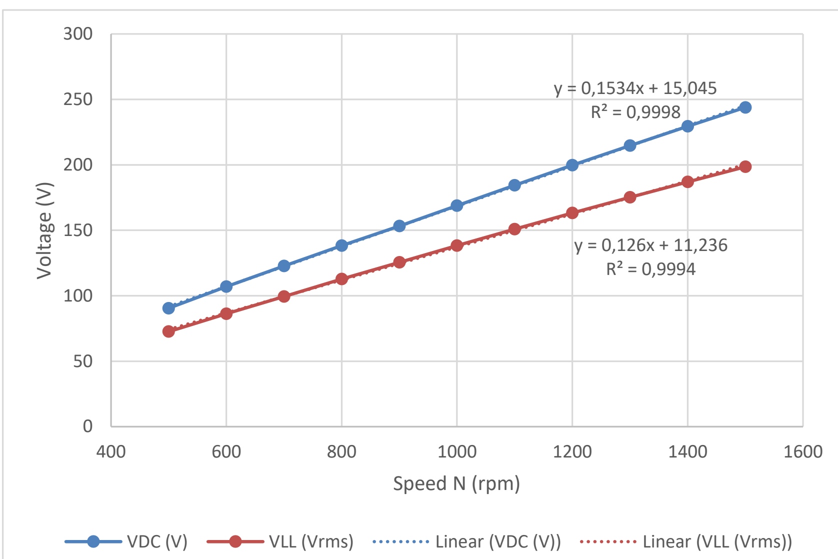

Figure 4.5: 60R110-4S3P-S-HP generator rated load test: V_{LL} and V_{DC} vs N.

The evolution of the continuous power (P_{DC}) in relation to the voltage V_{DC} is shown in Figure 4.6.

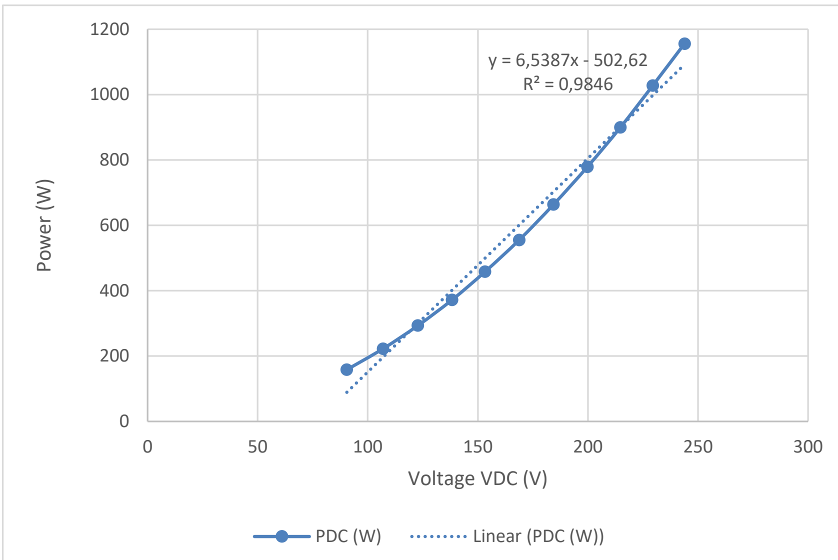

Figure 4.6: 60R110-4S3P-S-HP generator rated load test: P_{DC} vs V_{DC}.

The P_{DC} vs V_{DC} graph is not linear due to the voltage drop in the load. Excluding the voltage drop in the load impedance, it is expected a straight line, the coefficient of determination (R^2) is equals 0,9846.

4.1.3 Variable Load Test

In the variable load test, the intention is to keep the generator current set at the rated current (approximately 3,5 A), so that the generator always operates at full load. For this, when the speed is varied, the resistance load is varied proportionally, starting with 51,72 Ω. The setup used in this test is shown in Figure 4.7.

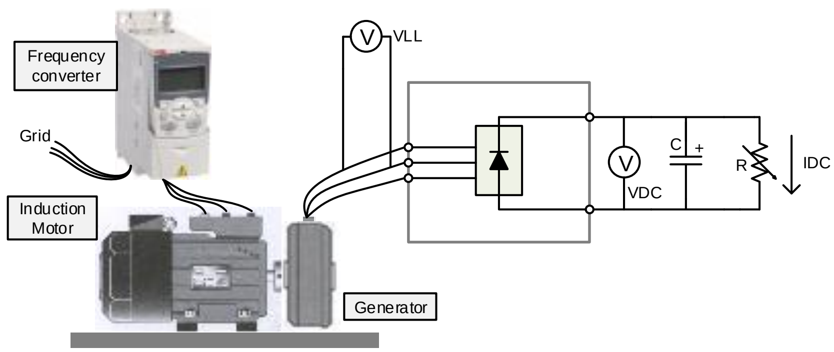

Figure 4.7: Variable load test setup.

The speed is decreased by a step of 100 rpm and the resistance is varied proportionally, thus maintaining the fixed current. The values measured in the variable load test are shown in Table 4.3.

Table 4.3: Variable load 60R110-4S3P-S-HP test.

N **[rpm]**	V_{LL} **[Vrms]**	I_g **[A]**	PF_g	P_g **[W]**	I_{DC} **[A]**	V_{DC} **[V]**	P_{DC} **[W]**
1500	198,5	3,5	0,95	1160	4,76	244	1161,44
1400	184,8	3,5	0,95	1080	4,76	226,8	1079,57
1300	171,1	3,5	0,95	1000	4,76	209,6	997,70
1200	157,5	3,5	0,95	920	4,76	192,5	916,30
1100	143,6	3,5	0,95	830	4,76	175,3	834,43
1000	130,2	3,5	0,95	760	4,76	158,6	754,94
900	116,7	3,5	0,95	680	4,76	141,6	674,02
800	103,1	3,5	0,95	600	4,76	124,8	594,05
700	89,4	3,5	0,95	520	4,77	107,8	514,21
600	75,9	3,5	0,94	440	4,76	91,2	434,11
500	62,4	3,5	0,94	360	4,76	74,4	354,14

At 1500 rpm, the dissipated power in the rheostat was approximately 1160 W. The Figure 4.8, shows the behavior of the voltages (V_{LL} and V_{DC}) in relation to the speed of the generator (N). As expected the relations are linear, with both coefficients of determination (R^2) equals 1.

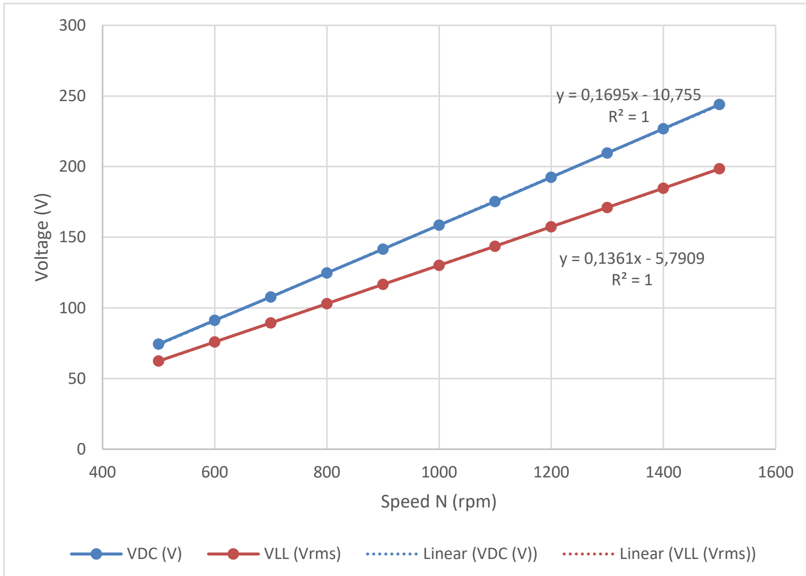

Figure 4.8: 60R110-4S3P-S-HP generator variable load: V_{DC} and V_{LL} vs N.

Figure 4.9 shows the relation between power (P_{DC}) and the direct voltage (V_{DC}). As expected the relation is linear, thus, the voltage is proportional to the generator speed (N), and the coefficient of determination (R^2) is equal to 1.

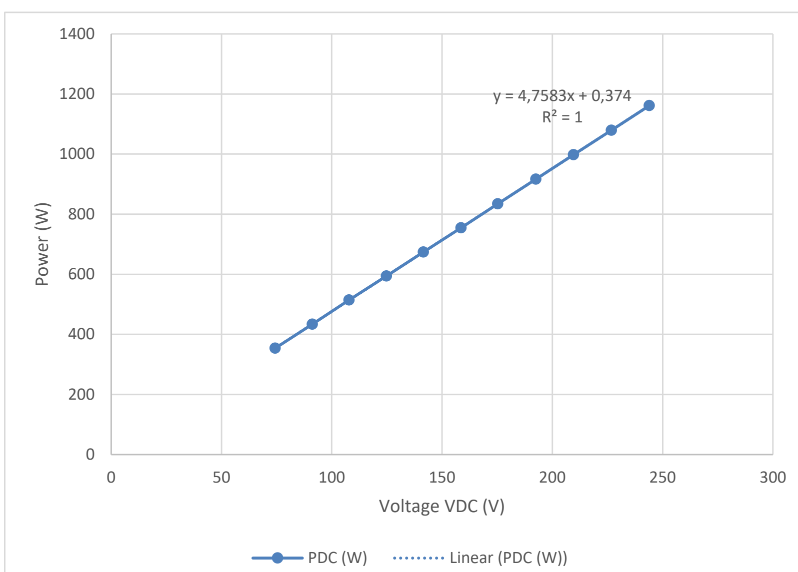

Figure 4.9: Variable load test with 60R110-4S3P-S-HP generator.

This test enables us to obtain the maximum power point (MPP) of the generator for a given DC voltage (proportional to the speed). Thus, the power line represented in Figure 4.9 is the MPP curve of the generator as a function of the speed. When a PV inverter is connected to a PMSG, it is expected the MPPT algorithm to follow this power line as will be presented in the next sections.

4.2 Grid-Connection Tests

Tests were carried out to evaluate the behavior of photovoltaic (PV) inverters in the connection to the grid of the pico-hydro turbines. The setup used for this test is shown in Figure 4.10.

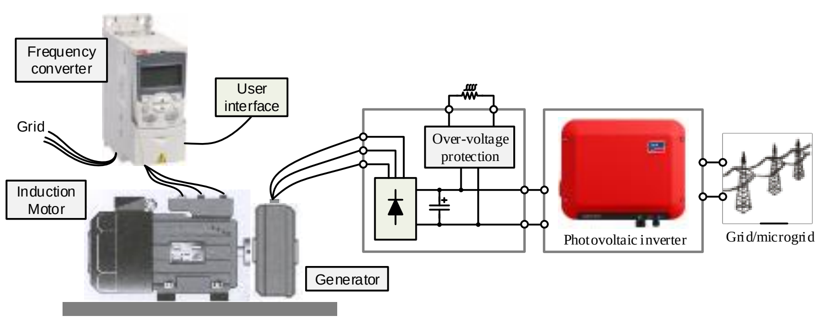

Figure 4.10: Grid connection test in laboratory.

The permanent magnet synchronous generator is coupled to the motor and connected to the protection circuit described in Section 3.6. The power clamp rectifies and controls the generator voltage to protect the PV inverters.

The frequency converter used in this test is an ACS 355-03E-07A3-4. The macro utilized is “PID Control” in power control mode, as will be presented in Subsection 4.2.1. Three PV inverters were used to test each PMSG, Sunny Boy 1.5-1VL-40, Omniksol-2k-TL2, and Sunny Boy 2100TL, described in Section 3.5.

In the grid-connection test, the parameters of the generators were measured, along with the input current and input voltage and the output power of the PV inverters. The speed of the motor-generator (N) was read in ACS355 keypad. The line-to-line voltages (V_{LL}), generator current (I_g), the generator power factor (PF_g) and the generator power (P_g) were measured with FLUKE 434 Power Quality Analyzer. The DC voltage of the PV inverter (V_{DC}) was measured with FLUKE 85 III True RMS Multimeter, the DC current of the PV inverter (I_{DC}) was measured with TES 2732 Multimeter.

This test was realized decreasing the power gradually. To test the LH400 turbine's generator, it was not necessary to use the protection circuit, because its no-load voltage is inferior that the maximum voltage supported by the inverters. On the contrary, to test the PLT350 HP, and TRG350 HP generators it was necessary to use the PowerClamp AC4 350-400, protection circuit.

4.2.1 ACS355 Parameters

In order to emulate the turbine as better as possible, the frequency converter controls the motor power, and therefore, the generator power. The physical connections of the ACS355 are shown in Figure 4.11.

1	SCR	Signal cable shield (screen)
2	AI1	**Proc. ref. (PID)/Motor freq. (Hand)**: 0...10 V [1]
3	GND	Analog input circuit common
4	+10 V	Reference voltage: +10 V DC, max. 10 mA
5	AI2	**Process actual value**: 4...20 mA[3] (motor power)
6	GND	Analog input circuit common
7	AO	**Motor power value**: 0...20 mA
8	GND	Analog output circuit common
9	+24 V	Auxiliary voltage output: +24 V DC, max. 200 mA

Figure 4.11: Physical connection in the ACS355. Adapted from [61].

The analog output is connected to the analog input 2 and both GND pins are connected. The most relevant groups of parameters utilized in this power control are described below.

Standard frequency converters are open programming devices. They can be used in a wide range of applications, therefore, they have a set of parameters, to suit each case. In addition, there are macros, with preprogrammed parameters, that enables rapid configuration for typical applications. The ACS355 macros are: ABB standard, 3-wire, alternate, motor potentiometer, hand/auto, PID control, torque control, ACS500 modbus. For the closed loop power control, the selected macro was PID control.

Group 99 - Start-up data

In group 99, the language and the motor parameters are defined, as well as the application macro used. The parameters values of group 99 are shown in Table 4.4.

Table 4.4: Group 99 - Start-up data.

Parameters	**Name**	**Project value**
9901	Language	English (0)
9902	Application macro	PID Control (6)
9903	Motor type	AM (1)
9904	Motor control type	Scalar:Frequency (3)
9905	Motor nominal voltage	400 V
9906	Motor nominal current	6,3 A
9907	Motor nominal frequency	50 Hz
9908	Motor nominal speed	1430 rpm
9909	Motor nominal power	3 kW
9912	Motor nominal torque	Read only
9913	Motor pole pairs	2
9915	Motor cos φ	0,84

The PID control was chosen to control the power of the motor in closed-loop, the suitable macro (PID) is defined in parameter 9902. The parameters 9903, 9905, 9906, 9907, 9908, 9909, 9913 and 9915 are motor specifications, described in Subsection 4.1.1. The type of motor control chosen was scalar control, in the parameter 9904. The motor torque is an option read only, in parameter 9012.

Group 40 - Process PID set 1

The group 40, is for the parametrization of the PID control variables. The Table 4.5 shows the selected project values.

Table 4.5: Group 40 - Process PID set 1.

Parameters	Name	Project value
4001	Gain	0,2
4002	Integration time	5 s
4003	Derivation time	0,0 s
4008	0% value	0
4009	100% value	100
4010	Setpoint select	Keypad (0)
4012	Setpoint min	0%
4013	Setpoint max	100%
4014	Feedback selection	ACT1 (1)
4016	ACT1 input	AI2 (2)
4017	ACT2 input	AI2 (2)
4018	ACT1 minimum	0%
4019	ACT1 maximum	100%

The gain and integration time, parameters 4001 and 4002, were achieved in trial and error approach, analyzing the response time and the stability of the system. The derivative component was not needed. The parameters 4008 and 4009 define the minimum and maximum PID values. The setpoint selection is made by keypad and the minimum and maximum values were set in parameter 4012 and 4013. The feedback selected is ACT1, the actual output value (output power). This measured output power is set in analog input 2. The minimum actual value selected is 0% and the maximum 100%.

Group 10 - Start/stop/direction

The sources for external start, stop and direction control are selected by the group 10. The parameters' values of group 10 are shown in Table 4.6.

The keypad was used for the start and stop control. The rotation direction of the motor is requested in initialization.

Table 4.6: Group 10 - Start/stop/direction.

Parameters	Name	Project value
1001	Ext1 commands	Keypad (8)
1002	Ext2 commands	Keypad (8)
1003	Direction	Request (3)

Group 11 - Reference select

The panel reference type, external control location, external reference sources and limits are defined in the group 11. The parameters values of this group are shown in Table 4.7.

Table 4.7: Group 11 - Reference select.

Parameters	Name	Project value
1101	Keypad reference select	REF2 (%) (2)
1102	EXT1/EXT2 select	EXT2 (7)
1103	REF1 select	Keypad (0)
1104	REF1 minimum	0 Hz
1105	REF1 maximum	50 Hz
1106	REF2 select	PID1 out (19)
1107	REF1 minimum	0%
1108	REF2 maximum	100%

For the PID control utilization, the keypad reference select was the REF2, the signal is in percentage. According to the PID control macro, the external control 2 (EXT2) was select. The keypad was chosen as signal source for the external reference 1 (REF1), with the minimum value of 0 Hz and the maximum of 50 Hz. The external reference 2 (REF2) signal source was the "PID1 controller" output with the minimum value of 0% and the maximum of 100%.

Group 13 - Analog inputs

In the group 13, the analog input signal processing is defined. The analog input 2 (current) is connected with the analog output. The Table 4.8 shows the selected values in the group 13.

Table 4.8: Group 13 - Analog inputs.

Parameters	Name	Project value
1304	Minimum AI2	0%
1305	Maximum AI2	100%

The analog input 1 it was not used, the analog input 2 minimum value set was 0% and the maximum value set was 100%.

Group 15 - Analog outputs

The selection of the actual signals (motor power, in this case) to be indicated through analog output and output signal processing, is defined in group 15. The values used in the test are shown in Table 4.9.

Table 4.9: Group 15 - Analog outputs.

Parameters	Name	Project value
1501	AO1 content select	Power (106)
1502	AO1 content minimum	0 kW
1503	AO2 content maximum	1,6 kW
1504	Minimum AO1	0A
1505	Maximum AO1	20mA

The parameter 1501 defines the power, as the signal to be obtained at the analog output AO1. The minimum and maximum value of analog output are set in the parameters 1502 and 1503. The minimum value for the analog output signal is set as 0 mA, in parameter 1504. The maximum value for the AO1 signal is set as 20 mA. The representation of the analog output is shown in Figure 4.12.

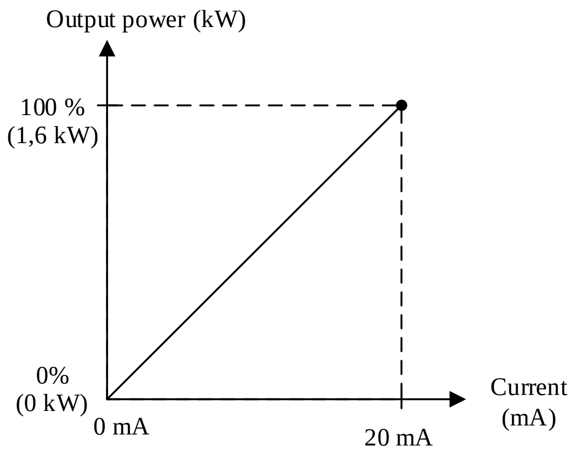

Figure 4.12: Analog output signal representation.

Group 20 - Limits

The speed and current limits are defined in the group 20. The used values are shown in Table 4.10

Table 4.10: Group 20 - Limits.

Parameters	Name	Project value
2001	Minimum speed	0 rpm
2002	Maximum speed	1700 rpm
2003	Maximum current	7,0 A

The speed range is selected in parameters 2001 and 2002, from 0 rpm to 1700 rpm. The motor current is limited in 7 A.

4.2.2 LH400 turbine's generator - 60R110-4S3P-S-HP

The LH400 turbine's generator, 60R1104S3P-S-HP, was tested in laboratory. The I_{DC} vs V_{DC} and P_{DC} vs V_{DC} graphs obtained with the acquired data are shown in Figure 4.13 and Figure 4.14, respectively.

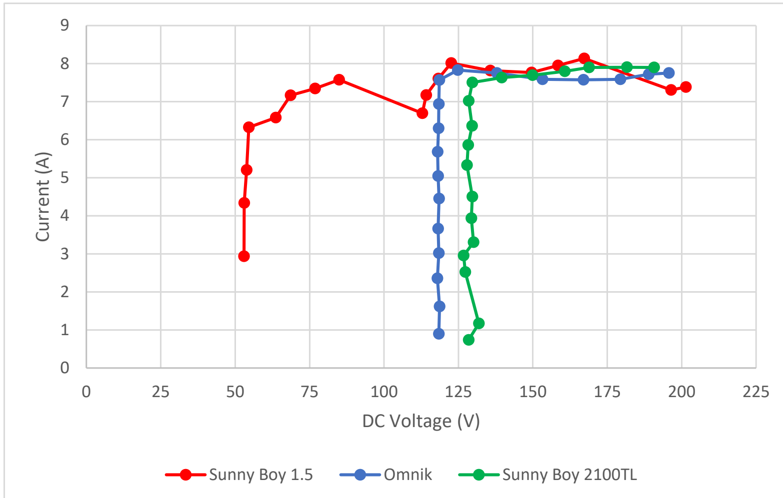

Figure 4.13: Grid-connection test of the generator 60R110-4S3P-S-HP, I_{DC} vs V_{DC} curves with different PV inverters.

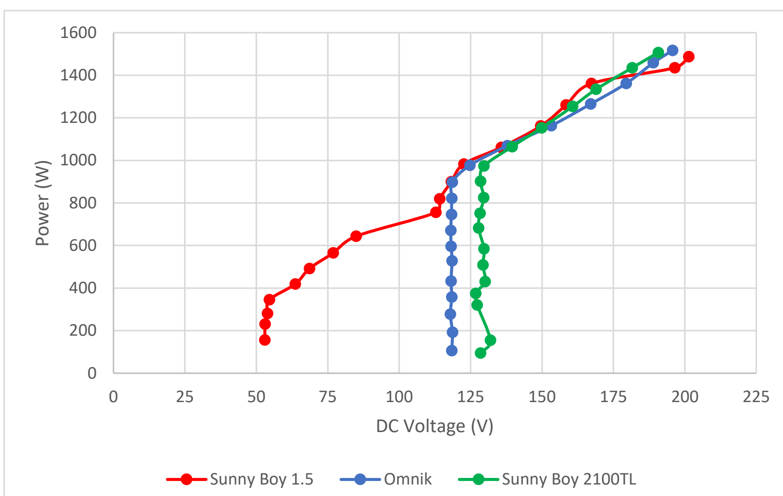

Figure 4.14: Grid-connection test of the generator 60R110-4S3P-S-HP, P_{DC} vs V_{DC} curves with different PV inverters.

In the current-voltage (I-V) graphs, it is possible to visualize the difference in the maximum power point track (MPPT) algorithm of the three PV inverters used. The MPPT algorithms controls the voltage and current values to try reach the maximum power point. Each inverter reaches a similar power in different zones of voltage (and consequently the current). The curves differ in minimum voltage of MPPT zone, that is described in Section 3.5. The minimum voltage of the Sunny Boy 2100TL MPPT range, is 125 V and 120 V for the Omniksol-2k-TL2. When the power falls below a certain value, they maintain the voltage and decrease the current. The Sunny Boy 1.5 has 160 V as the minimum value of MPPT range. However, when the power falls below 1300 W, the Sunny Boy 1.5 does not keep the voltage to 160 V, it maintains the current and decreases the voltage to near 50 V, the minimum operating voltage. In this case, the Sunny Boy 1.5 behave like the inferior limit of the MPPT range was 50V. The full data of this test are presented in Appendix A.

In the power-voltage curves, the three PV inverter curves are similar above the value of 1000 W. When the power falls below this value, as explained, the Sunny Boy 2100TL and Omniksol-2k-TL2 maintain the voltage in the inferior limit of the MPPT zone, and the Sunny Boy 1.5 does the same at 50 V.

4.2.3 PLT350 HP turbine's generator - 60R120-6S2P-S-HP

In the test using the PLT350 HP turbine's generator, 60R120-6S3P-S-HP, the same procedure of the LH440 generator test was used. Although, due to the high value of the 60R120-6S3P-S-HP open circuit voltage (Voc), it was necessary to use the protection circuit. The I_{DC} vs V_{DC} and the P_{DC} vs V_{DC} curves, with the measured values are presented in Figure 4.15 and Figure 4.16, respectively.

In the current-voltage and power-voltage graphs, the Sunny Boy 1.5 differs from the other two curves. In these conditions, it works with higher voltages, from 50 V to 325 V. It is possible to visualize that there are ups and downs in the current value in SB1.5 I-V curve. The Omniksol-2k-TL2 and Sunny Boy 2100Tl curves works between 120 V and 275 V, approximately. They work in a similar way, decreasing the voltage and keeping the current almost constant, when the power falls below 800 W, they stop decreasing the voltage, and begin decrease the current. It is important to understand that the power output of the three inverters is similar. The difference lies in the current-voltage pair, used to reach the power value.

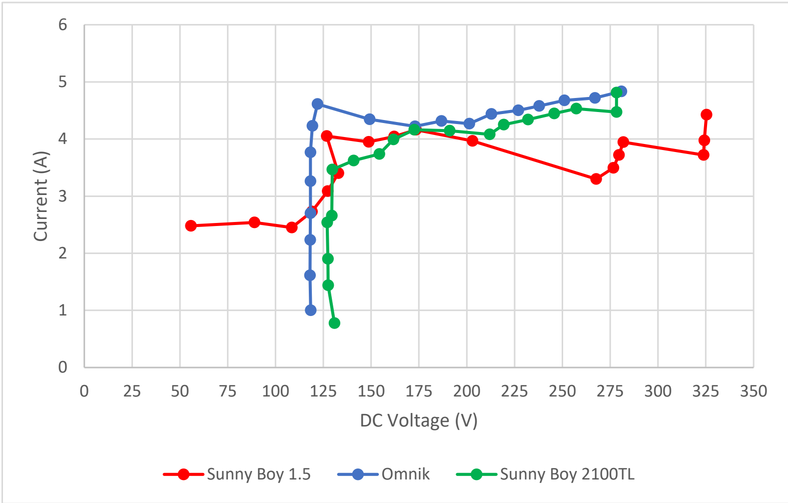

Figure 4.15: Grid-connection test of the generator 60R120-6S2P-S-HP, I_{DC} vs V_{DC} curves with different PV inverters.

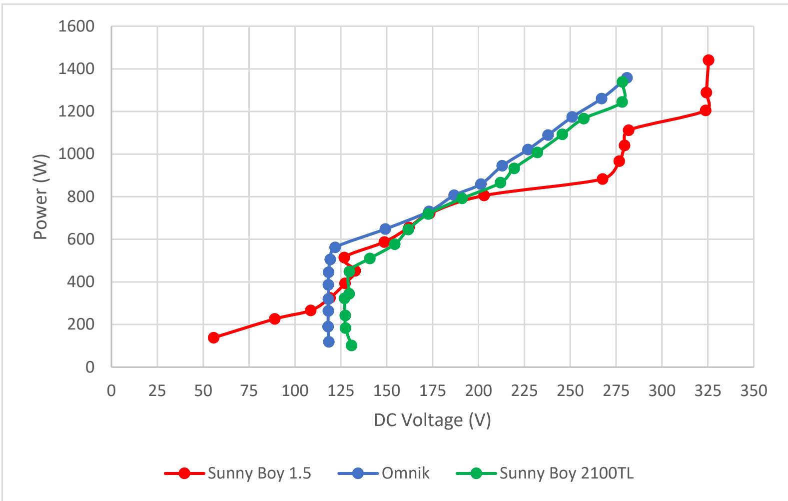

Figure 4.16: Grid-connection test of the generator 60R120-6S2P-S-HP, P_{DC} vs V_{DC} curves with different PV inverters.

As can be seen in Figure 4.16, with the Omniksol-2k-TL2 and Sunny Boy 2100TL PV inverters, the power behaves like a straight line, within the MPPT range. This is expected considering the results shown in Figure 4.9.

4.2.4 TRG350 HP turbine's generator - 60R90-6S2P-S-HP

In the TRG350 HP turbine's generator test, likewise the PLT350 HP turbine's generator test, it was necessary the utilization of the protection circuit (described in Section 3.6). The open circuit voltage of this generator is higher than the three photovoltaic inverters support, and can reach close to 720 V. The I_{DC} vs V_{DC} and P_{DC} vs V_{DC} curves of this test are shown in Figures 4.17 and 4.18, respectively. The data obtained with the three PV inverters, Sunny Boy 1.5, Omniksol-2k-TL2 and Sunny Boy 2100TL are presented in Tables A.7, A.8 and A.9, respectively.

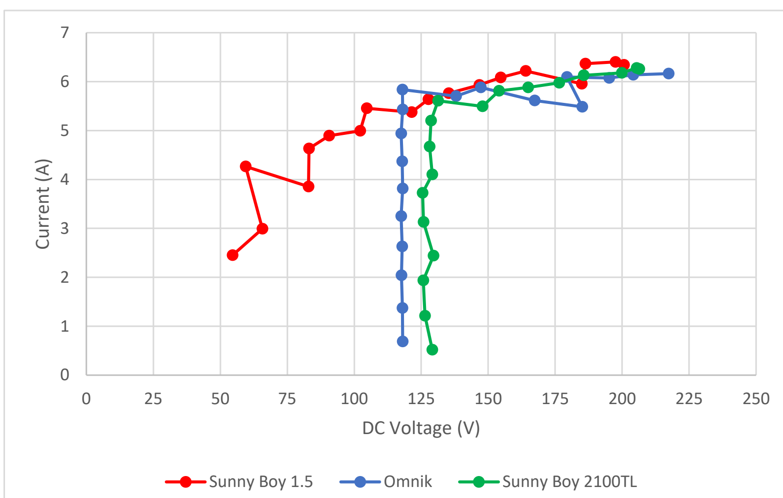

Figure 4.17: Grid-connection test of the generator 60R90-6S2P-S-HP, I_{DC} vs V_{DC} curves with different PV inverters.

The Sunny Boy 1.5 also has a higher range of voltage than the other two PV inverters, from 50 V to 200 V. The current range of SB 1.5 is from approximately 2,5 A and 6,5 A. The Omniksol-2k-TL2 and the Sunny Boy 2100TL have similar curves both in I_{DC} vs

V_{DC}, and in P_{DC} vs V_{DC}, with a smaller range in voltage, and a higher range in current than the Sunny Boy 1.5 curve.

It should be highlighted that, in this case, the maximum power curve, obtained with all inverters within their MPPT range, follows the behavior identified in Figure 4.9.

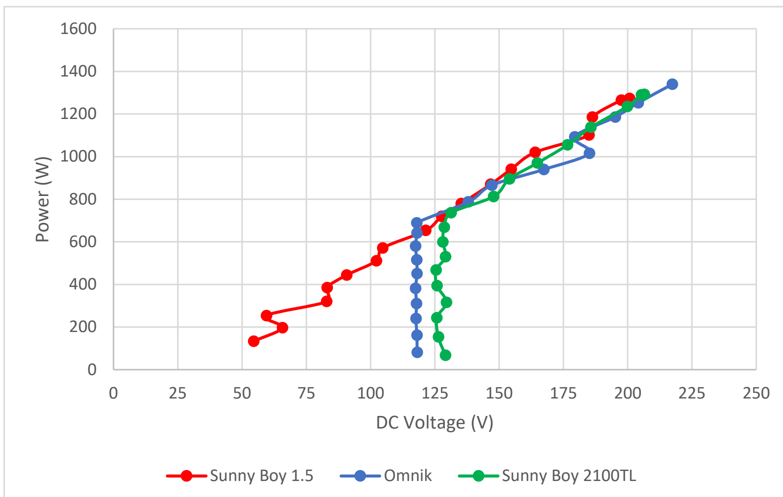

Figure 4.18: Grid-connection test of the generator 60R90-6S2P-S-HP, P_{DC} vs V_{DC} curves with different PV inverters.

4.3 Turbine Tests

The real condition tests with the turbines were conducted in the experimental platform described in Chapter 3. The tests were carried out controlling the pump through frequency, with a step of 2,5 Hz, measuring the values of flow or pressure, I_{DC}, V_{DC} and P_{AC}. The P_{DC} was calculated using I_{DC} and V_{DC}. It was made an average value of three samples. The full data of this test is presented in Appendix B.

4.3.1 System 1: Low Heads

In the System 1 test, the head is fixed in 4,4 m, the water flow was varied through the ACS355's frequency. The variables measured were flow, I_{DC}, V_{DC} and P_{AC}. In this test, it was used two PV inverters to the grid-connection, Omniksol-2k-TL2 and Sunny Boy 2100TL. The test with the Sunny Boy 1.5 inverter was not successfully achieved, the inverter did not come into operation. The full data table of the test with the LH400 in the platform is presented in Tables B.1 and B.2. The I_{DC} vs V_{DC} curve of LH400 turbine test in the platform is shown in 4.19.

The Omniksol-2k-TL2 curve behaves like in the grid-connecting test, presented in Figure 4.13, except in a point, and the lower number of samples. The Sunny Boy 2100TL curve in the real condition test does not approximate the grid-connecting test curve obtained with the turbine emulation. The I-V curves are achieved through the work of the PV inverters MPPT algorithm and the way that current and voltage are varied are unknown. The P_{DC} vs V_{DC} curves of the LH400 using the PV inverters are shown in Figure 4.20.

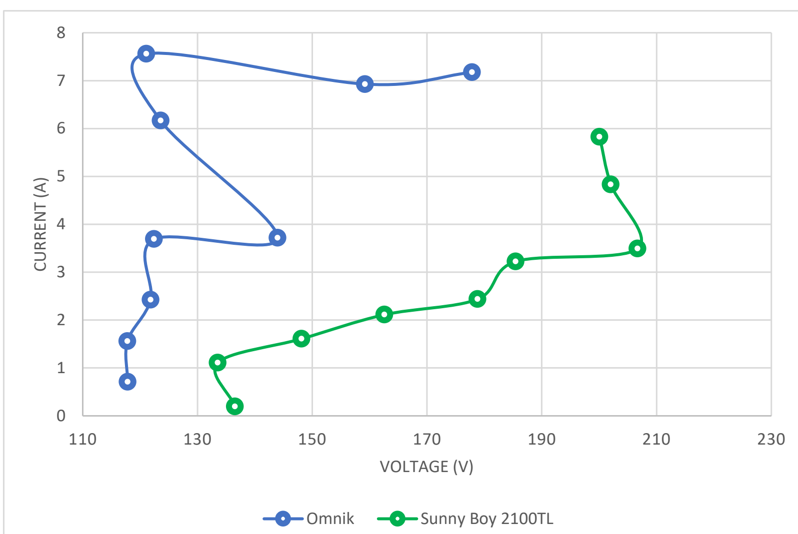

Figure 4.19: LH400 platform test, I_{DC} vs V_{DC} curve.

In the power-voltage graph it is possible to visualize that using different operating modes of the MPPT algorithm, a nearby power can be reached. The P_{DC} vs flow rate (Q) is shown in Figure 4.21.

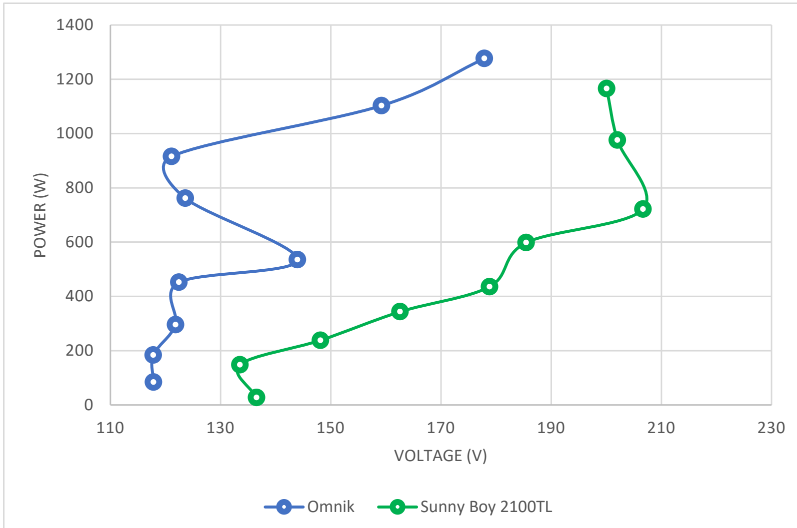

Figure 4.20: LH400 platform test, P_{DC} vs V_{DC} curve.

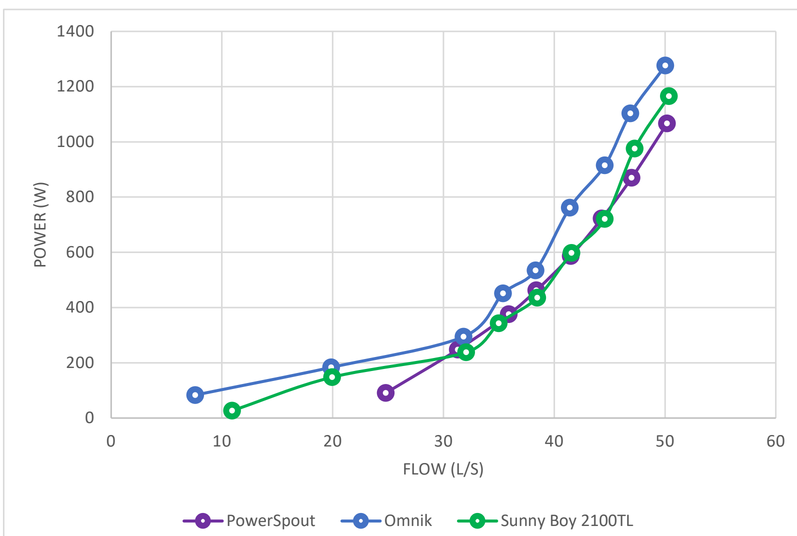

Figure 4.21: LH400 platform test, P_{DC} vs Q curve.

The power-flow curve is presented along with the theoretical values, in purple. The theoretical values were taken from the table "Flow calculations and generation options" of the LH400 turbine installation manual [52]. It is important to note that in the manual table, the flow is imposed by the head. In the test done, the head is fixed.

The curves reached in the test are similar to the theoretical curves. This shows that the conditions created on the platform are close to actual operating conditions of the PowerSpout LH400 propeller turbine.

The turbine LH400, will be used in the projects of House of Silk and the Castrelos Aquaculture Centre. Considering the compatibility between the 60R110-4S3P-S-HP generator and the PV inverters, based on the results of the turbine tests, the most recommended would be the Omniksol-2k-TL2. The obtained results with the Sunny Boy 2100TL were also satisfactory. At first, the PV inverter Sunny Boy 1.5 would not work, considering the integration aspects of both projects.

4.3.2 System 2: Heads Emulation

In the system 2 tests, the original idea was to measure the pressure and the flow rate. However, due to mechanical problems in the flow rate sensor, it was not possible to acquire the flow data. This problem does not affect the consistency and validation of the test, since the main variable is the pressure. This tests were made with the three inverters, Sunny Boy 1.5, Omniksol-2k-TL2 and Sunny Boy 2100TL. The ACS355 controls the frequency of the Helix V pump, and the step chosen was 2,5 Hz. The PLT350 HP and the TRG350 HP tests were made in the same configuration.

PLT350 HP turbine

The PLT350 HP was tested with Sunny Boy 1.5, Omniksol-2k-TL2 and Sunny Boy 2100TL. The full data of this test is presented in Tables B.3, B.4 and B.5, respectively. The I_{DC} vs V_{DC} curves of the three PV inverters are shown in the Figure 4.22. The P_{DC} vs V_{DC} curves are presented in Figure 4.23.

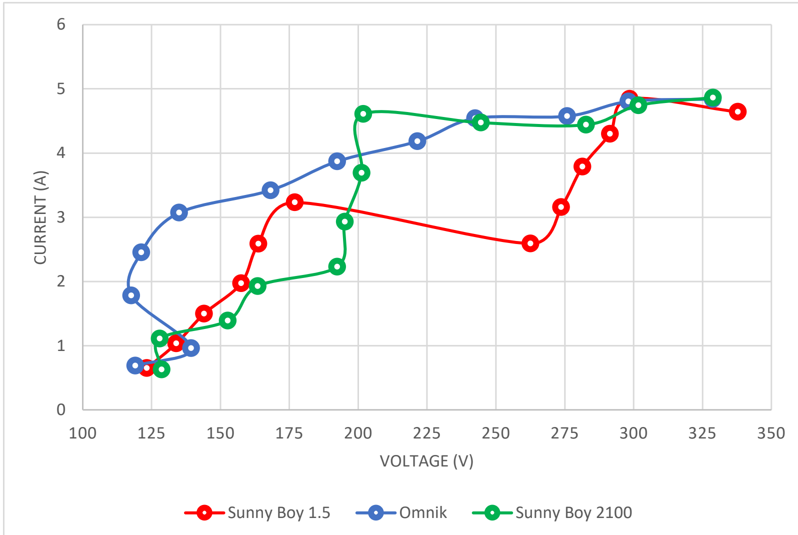

Figure 4.22: PLT350 HP platform test I_{DC} vs V_{DC}.

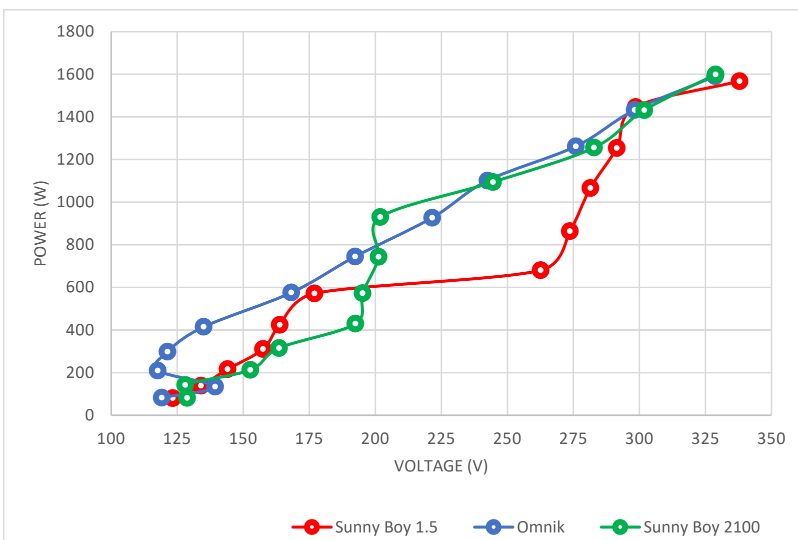

Figure 4.23: PLT350 HP platform test P_{DC} vs V_{DC}.

In the platform test with the PLT350 HP turbine, the three I-V curves have the same range of voltage and current, unlike the generator grid-connection test. As in the other tests, the current-voltage pairs of the inverters travel different paths for similar power values. In the Sunny Boy 1.5 curve, there is a sudden drop in voltage, almost 100 V. However, the difference between the power of the two points is similar to that of the two other PV inverters.

In this test, the I-V working course is different from the obtained results in the power control grid-connection test (turbine emulation). However, the power-voltage curve behaves as expected. With the three PV inverters used, within its MPPT range, power follows approximately a straight line.

The Figure 4.24 shows the P_{DC} vs Pressure curves in the PLT350 HP tests.

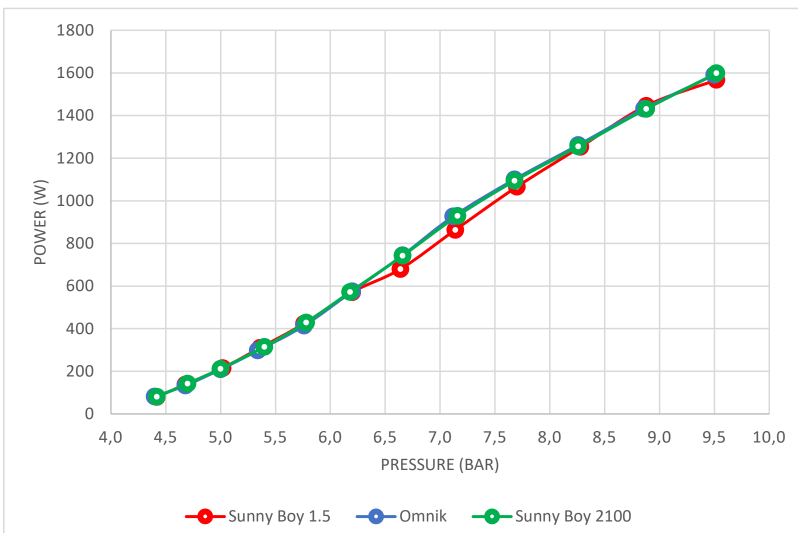

Figure 4.24: PLT350 HP platform test P_{DC} vs Pressure.

The three PV inverters curves, in the P_{DC} vs pressure graphs, are practically overlapped. This indicates that even with different I-V curves, with similar pressures, the three inverters reach the same power.

TRG350 HP turbine

The TRG350 HP platform tests, were performed with the Sunny Boy 1.5, Omniksol-2k-TL2 and Sunny Boy 2100TL, the full measured values are presented in Tables B.6, B.7 and B.8, respectively. The obtained curves of I_{DC} vs V_{DC} of the TRG350 HP platform test, is shown in Figure 4.25.

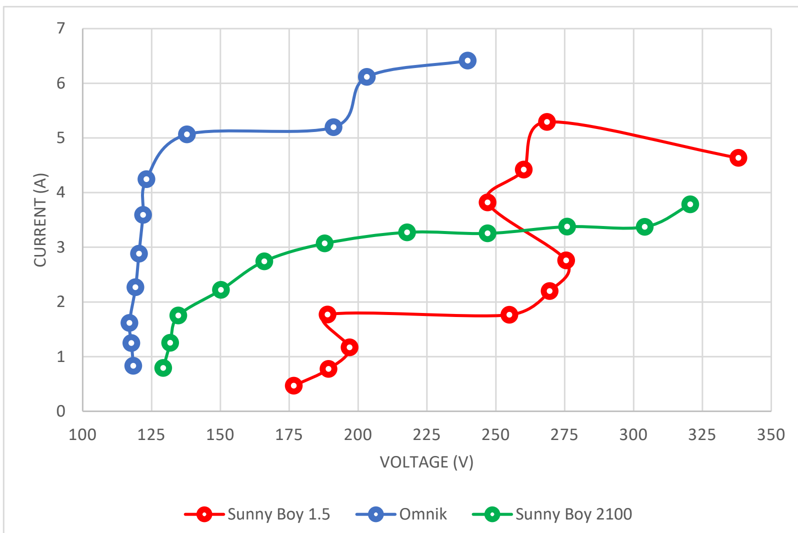

Figure 4.25: TRG350 HP platform test I_{DC} vs V_{DC}.

In this case, the three inverters work within their MPPT range. The Omniksol-2k-TL2 works in the zone between 120 V and 245 V approximately. The Sunny Boy 1.5 works between 175 V and 340 V and the Sunny Boy 2100TL works between 130 V and 320 V. The current in the Sunny Boy 2100TL does not exceed 4 A, while Omniksol-2k-TL2 reach 6,4 A and the Sunny Boy 1.5 reach 5,3 A. The figure 4.26 shows the P_{DC} vs V_{DC} curves and the P_{DC} vs pressure curves of the TRG350 HP are shown in Figure 4.27.

In this test the PV inverter Sunny Boy 1.5 obtained better power values compared to similar pressures than the other two inverters.

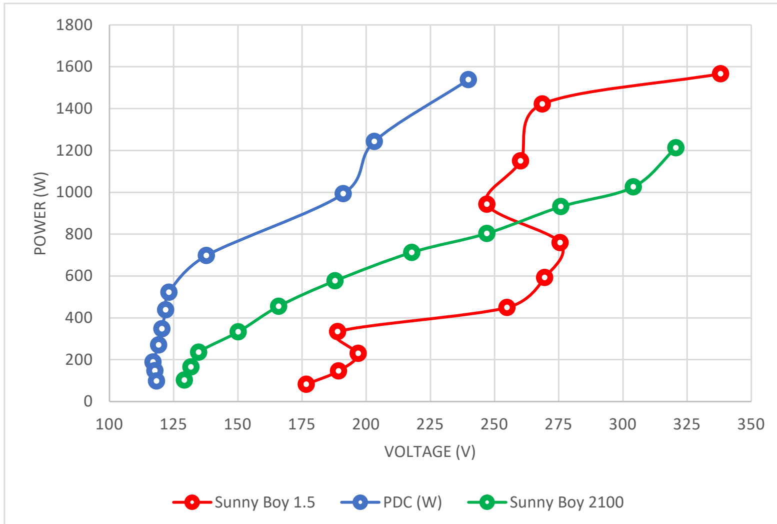

Figure 4.26: TRG350 HP platform test P_{DC} vs V_{DC}.

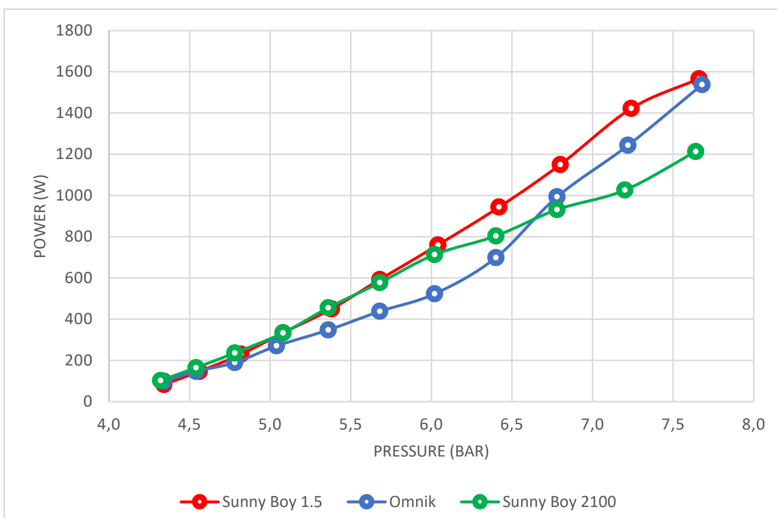

Figure 4.27: TRG350 HP platform test P_{DC} vs Pressure.

Although, due to a mechanical problem with turgo turbine, there is a difference of 400 W between the power achieved with Sunny Boy 2100TL and the other two inverters. The power of Sunny Boy 2100TL does not exceed 1,2 kW, while the other two PV inverters reach a maximum power of approximately 1,5 kW. The problem is clearly viewed in pressures over 6 bar, on P_{DC} vs pressure graph. The problem could not be solved in time for further testing with the Sunny Boy 2100TL PV inverter.

The obtained results are very relevant since it guarantees, in real conditions, the compatibility of PV inverters with hydro-turbines. These results demonstrate that, in many cases, PV inverters can be used efficiently in pico-hydro systems.

Chapter 5

Conclusions and Further Work

This chapter presents the main conclusions and further work suggestions about the design, implementation, and tests of the experimental platform for emulation of pico-hydro systems connected to the grid.

5.1 Conclusions

It was implemented an experimental platform for emulation of pico-hydro turbines, focused on the grid-connection of these systems. With educational and applied research purposes, besides helping the development of ongoing projects, namely, House of Silk and Castrelos Aquaculture Centre.

Three systems were implemented in the platform, a system of low heads (up to 5 m), with a test performed with a propeller turbine. A system for heads emulation with Pelton and turgo turbines. A system for the test of a horizontal water wheel.

Laboratory tests were carried out to characterize the turbine used in the projects, the emulation of the turbines in the grid connection and tests under real conditions in the platform.

It was necessary to overcome many adversities, among them the delay in the delivery of the equipment, coming from New Zealand, difficulty in the construction and sealing of the flume and difficulty of assembling the tubes for very high pressures.

The PowerSpout LH400 low head turbine test presented satisfactory results when compared to the data provided by the manufacturer. The compatibility of the turbine with the photovoltaic inverters Sunny Boy 2100TL and Omniksol-2k-TL2 was validated.

The heads emulation test with PowerSpout's HP PLT350 HP and TRG350 HP turbines presented satisfactory results. The PLT350 HP turbine achieved better results when compared to the TRG350 HP turbine due to mechanical problems. The compatibility of both turbines with the three grid interface photovoltaic inverters tested, Sunny Boy 1.5, Omniksol-2k-TL2 and Sunny Boy 2100TL, was validated. The overvoltage control with the protection circuit was also evaluated and it proved to be efficient.

5.2 Further Work

This work has the potential to be continued. As future work, the improvement of the mechanical installations in the low heads system, in order to provide tests at variable heads. The test of other types of turbines, such as cross-flow, Francis, Kaplan and water wheels is also suggested. The closed loop control of flow rate as the process variable, in the low head system, and pressure for head emulation system should also be further investigated.

Bibliography

[1] U. Nations, "The future energy matrix and renewable energy: Implications for energy and food security", in *Trade and Development Commission - Multi-year Expert Meeting on Commodities and Development*, 2010.

[2] A. Chakraborty, "Advancements in power electronics and drives in interface with growing renewable energy resources", *Renewable and Sustainable Energy Reviews*, vol. 15, no. 4, pp. 1816–1827, 2011, ISSN: 1364-0321. DOI: `https://doi.org/10.1016/j.rser.2010.12.005`.

[3] I. E. Agency, *Energy access otlook 2017 - from poverty to prosperity*. [Online]. Available: `https://bit.ly/2zRFdZ8` (visited on 10/21/2018).

[4] M. F. Basar, A. Ahmad, N. Hasim, and K. Sopian, "Introduction to the pico hydro power and the status of implementation in malaysia", in *2011 IEEE Student Conference on Research and Development*, Dec. 2011, pp. 283–288. DOI: `10.1109/SCOReD.2011.6148751`.

[5] V. Leite, J. Couto, Â. Ferreira, and J. Batista, "A practical approach for grid-connected pico-hydro systems using conventional photovoltaic inverters", in *2016 IEEE International Energy Conference (ENERGYCON)*, Apr. 2016, pp. 1–6. DOI: `10.1109/ENERGYCON.2016.7513911`.

[6] W. Maidana, V. Leite, A. Ferreira, L. Queijo, J. Batista, J. Bonaldo, and E. Goncalves, "Design of a self-sustainable system based on renewable energy sources for a small museum of science dissemination - the house of silk", in *III Congresso Ibero-Americano de Empreendedorismo, Energia, Ambiente e Tecnologia - CIEEMAT 2017*, Jul. 2017.

[7] W. E. Council. (2016). World energy resources | 2016, [Online]. Available: `https://bit.ly/2Jq9BLx` (visited on 05/22/2018).

[8] K. Sopian and J. Razak, "Pico hydro: Clean power from small streams", in *Proceedings of the 3rd World Scientific and Engineering Academy and Society International Conference on Renewable Energy Sources, Tenerife, Spain*, vol. 13, 2009.

[9] A. Williams and R. Simpson, "Pico hydro–reducing technical risks for rural electrification", *Renewable Energy*, vol. 34, no. 8, pp. 1986–1991, 2009.

[10] N. El Bassam and P. Maegaard, *Integrated renewable energy for rural communities: Planning guidelines, technologies and applications*. Elsevier, 2004.

[11] A. Harvey, *Micro-hydro design manual: A guide to small-scale water power schemes.* 621.24/H341. Intermediate Technology Publications, 1993.

[12] S. J. Williamson, A. Griffo, B. H. Stark, and J. D. Booker, "Control of parallel single-phase inverters in a low-head pico-hydro off-grid network", in *IECON 2013 - 39th Annual Conference of the IEEE Industrial Electronics Society*, Nov. 2013, pp. 1571–1576. DOI: `10.1109/IECON.2013.6699367`.

[13] P. Action, "Micro-hydro power", *Fact Sheet*, 2014.

[14] R. Sturdivant, J. Yeh, M. Stambaugh, A. Zahnd, and E. K. P. Chong, "Pico-hydro electric power in the nepal himalayas", in *2017 Ninth Annual IEEE Green Technologies Conference (GreenTech)*, Mar. 2017, pp. 232–237. DOI: `10.1109/GreenTech.2017.40`.

[15] V. Leite, Â. P. Ferreira, J. Couto, and J. Batista, "Pico-hydro systems: Microgrid-connection approaches", in *IV Congreso Iberoamericano Sobre Microrredes con Generación Distribuida de Renovables*, 2016.

[16] V. Leite, Â. Ferreira, J. Couto, and J. Batista, "Compatibility analysis of grid-connected pico-hydro systems using conventional photovoltaic inverters", in *2016 18th European Conference on Power Electronics and Applications (EPE'16 ECCE Europe)*, Sep. 2016, pp. 1–9. DOI: `10.1109/EPE.2016.7695615`.

[17] A. Zahnd, K. Mckay, and R. Komp, "Renewable energy village power systems for remote and impoverished himalayan villages in nepal", 2006.

[18] N. Smith and G. Ranjitkhar, "Nepal case study–part one: Installation and performance of the pico power pack", *Pico Hydro Newsletter*, pp. 2–4, 2000.

[19] M. A. A. Syed, M. M. N. Ali, F. S. Hossain, S. A. Haque, and A. H. Siddique, "Prospect of a pico hydro power plant based on irrigation pump in perspective of rural areas in bangladesh", in *2011 2nd International Conference on Electric Power and Energy Conversion Systems (EPECS)*, Nov. 2011, pp. 1–6. DOI: `10.1109/EPECS.2011.6126793`.

[20] D. Howey, "Axial flux permanent magnet generators for pico-hydropower", in *EWB-UK research conference*, Citeseer, vol. 20, 2009.

[21] M. R. F. Machado, "Microturbinas em redes de abastecimento de água", Master's thesis, Universidade de Aveiro, 2015.

[22] I. E. Agency, "Small-scale hydro within a municipal water supply system", CADDET Renewable Energy, Tech. Rep., 1998.

[23] R. K. Saket, "Design, development and reliability evaluation of micro hydro power generation system based on municipal waste water", in *2008 IEEE Canada Electric Power Conference*, Oct. 2008, pp. 1–8. DOI: `10.1109/EPC.2008.4763355`.

[24] M. Silva, V. Leite, P. Araujo, A. Simoes, I. Dalmarco, A. Ferreira, and L. Queijo, "Designing innovative home energy systems for smart cities: The silkhouse project", in *I Ibero-American Congress of Smart Cities (ICSC-CITIES 2018)*, Sep. 2018.

[25] M. Silva, V. Leite, D. Roman, P. Araujo, W. Maidana, and J. Batista, "Design of a microgrid based on renewable energy sources for an aquaculture centre", in *I Ibero-American Congress of Smart Cities (ICSC-CITIES 2018)*, Sep. 2018.

[26] Y. A. Cengel and J. M. Cimbala, *Fluid mechanics fundamentals and applications*. 2006, vol. 185201.

[27] C. Warnick, *Hydropower engineering*. Prentice-Hall Incorporated, Englewood Cliffs, NJ, USA, 1984.

[28] T. K. Ghosh and M. A. Prelas, *Energy resources and systems: Volume 2: Renewable resources*. Springer Science & Business Media, 2011, vol. 2.

[29] O. Paish, "Micro-hydropower: Status and prospects", *Proceedings of the Institution of Mechanical Engineers, Part A: Journal of Power and Energy*, vol. 216, no. 1, pp. 31–40, 2002.

[30] D. K. Okot, "Review of small hydropower technology", *Renewable and Sustainable Energy Reviews*, vol. 26, pp. 515–520, 2013.

[31] S. Sangal, A. Garg, and D. Kumar, "Review of optimal selection of turbines for hydroelectric projects", *International Journal of Emerging Technology and Advance Engineering*, vol. 3, pp. 424–430, 2013.

[32] U. D. of Energy, *Types of hydropower turbines*. [Online]. Available: `https://bit.ly/2PlfjSz` (visited on 08/30/2018).

[33] A. Elbatran, O. Yaakob, Y. M. Ahmed, and H. Shabara, "Operation, performance and economic analysis of low head micro-hydropower turbines for rural and remote areas: A review", *Renewable and Sustainable Energy Reviews*, vol. 43, pp. 40–50, 2015.

[34] B. R. Cobb and K. V. Sharp, "Impulse (turgo and pelton) turbine performance characteristics and their impact on pico-hydro installations", *Renewable Energy*, vol. 50, pp. 959–964, 2013.

[35] S. J. Williamson, B. H. Stark, and J. D. Booker, "Experimental optimisation of a low-head pico hydro turgo turbine", in *2012 IEEE Third International Conference on Sustainable Energy Technologies (ICSET)*, Sep. 2012, pp. 322–327. DOI: `10.1109/ICSET.2012.6357419`.

[36] W. R. Energy, *Gallery*. [Online]. Available: `https://bit.ly/2SqRSJq` (visited on 08/31/2018).

[37] A. Hughes and W. Drury, *Electric motors and drives: Fundamentals, types and applications*. Newnes, 2013.

[38] S. Chapman, *Electric machinery fundamentals*. Tata McGraw-Hill Education, 2011.

[39] F. Schwartz, R. Pegallapati, and M. Shahidehpour, "Small hydro as green power", in *IEEE Power Engineering Society General Meeting, 2005*, Jun. 2005, 2050–2057 Vol. 2. DOI: 10.1109/PES.2005.1489455.

[40] A. E. Fitzgerald, C. Kingsley, S. D. Umans, and B. James, *Electric machinery*. McGraw-Hill New York, 2003, vol. 5.

[41] T. Ackermann, *Wind power in power systems*. John Wiley & Sons, 2005.

[42] J. A. P. P. Brás, "Interface de um gerador eólico para microgeração de energia com cargas eléctricas", Master's thesis, Universidade do Minho, 2011.

[43] T. Ackermann, G. Andersson, and L. Söder, "Distributed generation: A definition", *Electric Power Systems Research*, vol. 57, no. 3, pp. 195–204, 2001, ISSN: 0378-7796. DOI: https://doi.org/10.1016/S0378-7796(01)00101-8.

[44] A. B. Rújula, J. M. Amada, J. Bernal-Agustin, J. Y. Loyo, and J. D. Navarro, "Definitions for distributed generation: A revision", in *International Conference on Renewable Energy and Power Quality March*, 2005, pp. 16–18.

[45] J. M. Guerrero, F. Blaabjerg, T. Zhelev, K. Hemmes, E. Monmasson, S. Jemei, M. P. Comech, R. Granadino, and J. I. Frau, "Distributed generation: Toward a new energy paradigm", *IEEE Industrial Electronics Magazine*, vol. 4, no. 1, pp. 52–64, Mar. 2010, ISSN: 1932-4529. DOI: 10.1109/MIE.2010.935862.

[46] M. G. Molina and M. Pacas, "Improved power conditioning system of micro-hydro power plant for distributed generation applications", in *2010 IEEE International Conference on Industrial Technology*, Mar. 2010, pp. 1733–1738. DOI: 10.1109/ICIT.2010.5472461.

[47] F. Blaabjerg, R. Teodorescu, M. Liserre, and A. V. Timbus, "Overview of control and grid synchronization for distributed power generation systems", *IEEE Transactions on Industrial Electronics*, vol. 53, no. 5, pp. 1398–1409, Oct. 2006, ISSN: 0278-0046. DOI: `10.1109/TIE.2006.881997`.

[48] U. D. of Energy, *Off-grid or stand-alone renewable energy systems*. [Online]. Available: `https://bit.ly/2RnNiKH` (visited on 09/22/2018).

[49] ——, *Grid-connected renewable energy systems*. [Online]. Available: `https://bit.ly/2RhPpj5` (visited on 09/25/2018).

[50] K. S. Krishna and K. S. Kumar, "A review on hybrid renewable energy systems", *Renewable and Sustainable Energy Reviews*, vol. 52, pp. 907–916, 2015, ISSN: 1364-0321. DOI: `https://doi.org/10.1016/j.rser.2015.07.187`.

[51] M. Jayachandran and G. Ravi, "Design and optimization of hybrid micro-grid system", *Energy Procedia*, vol. 117, pp. 95–103, 2017, ISSN: 1876-6102. DOI: `https://doi.org/10.1016/j.egypro.2017.05.111`.

[52] PowerSpout, *Powerspout document index links*. [Online]. Available: `https://bit.ly/2buQUdK` (visited on 09/30/2018).

[53] Grundfos, *Grundfos data booklet - flow sensors*. [Online]. Available: `https://bit.ly/2RiQPKg` (visited on 09/30/2018).

[54] Wilo, *Cronobloc-bl 125/185-5,5/4*. [Online]. Available: `https://bit.ly/2Dd0UFs` (visited on 09/30/2018).

[55] S. Electric, *Grundfos data booklet - flow sensors*. [Online]. Available: `https://bit.ly/2Rnu33X` (visited on 09/30/2018).

[56] Wilo, *Helix v 3604-1/16/e/ks*. [Online]. Available: `https://bit.ly/2DaEZPj` (visited on 09/30/2018).

[57] I. Dalmarco, P. Araujo, V. Leite, L. Queijo, and L. Lima, "Prototyping a horizontal water wheel for electricity generation in a small museum: The house of silk", in *I Ibero-American Congress of Smart Cities (ICSC-CITIES 2018)*, Sep. 2018.

[58] SMA, *Sunny boy 1.5/2.5*. [Online]. Available: https://bit.ly/2Q2dUQU (visited on 10/19/2018).

[59] O. N. Energy, *Omniksol-1k/1.5k/2k-tl2*. [Online]. Available: https://bit.ly/2PtWujk (visited on 10/19/2018).

[60] SMA, *Operating manual - sunny boy 1300tl / 1600tl / 2100tl*. [Online]. Available: https://bit.ly/2PqrUXD (visited on 10/19/2018).

[61] ABB, *Users manual acs355 drives*. [Online]. Available: https://bit.ly/2D3NWts (visited on 09/30/2018).

Appendix A

Grid-Connection Tests Full Data

Table A.1: Grid-connection test with generator 60R110-4S3P-S-HP and Sunny Boy 1.5.

N [rpm]	$\mathbf{V}_{LL}$ [Vrms]	$\mathbf{I}_g$ [A]	$\mathbf{PF}_g$	$\mathbf{P}_g$ [W]	$\mathbf{I}_{DC}$ [A]	$\mathbf{V}_{DC}$ [V]	$\mathbf{P}_{DC}$ [W]	
1485,00	163,20	5,47	0,97	1.490,0	201,40	7,38	1486,94	1,41
1454,67	160,25	5,43	0,97	1.460,0	196,47	7,30	1435,12	1,37
1365,33	136,73	6,03	0,97	1.380,0	167,27	8,14	1360,99	1,29
1276,00	133,67	5,73	0,97	1.280,0	158,43	7,95	1259,97	1,20
1187,00	120,43	5,83	0,97	1.180,0	149,57	7,76	1161,24	1,11
1104,00	112,53	5,80	0,96	1.090,0	135,73	7,82	1061,25	1,01
1018,00	97,37	6,13	0,96	1.000,0	122,60	8,01	982,52	0,92
945,00	97,33	5,63	0,96	920,0	118,27	7,61	899,81	0,84
877,67	94,23	5,37	0,96	840,0	114,20	7,17	819,19	0,77
827,67	65,83	4,90	0,96	770,0	112,83	6,70	755,42	0,70
705,67	72,60	5,50	0,96	660,0	84,93	7,58	643,51	0,60
628,67	63,57	5,53	0,96	580,0	76,87	7,35	564,71	0,52
558,00	57,27	5,27	0,96	510,0	68,57	7,17	491,39	0,45
495,00	52,43	5,00	0,96	430,0	63,63	6,58	418,71	0,38
424,00	43,07	5,10	0,96	360,0	54,60	6,33	345,44	0,31
387,00	47,10	3,83	0,95	300,0	53,87	5,20	280,29	0,25
357,33	31,99	3,10	0,94	230,0	53,07	4,34	230,31	0,19
329,00	45,20	2,20	0,93	160,0	52,97	2,94	155,55	0,14

Table A.2: Grid-connection test with generator 60R110-4S3P-S-HP and Omnik.

N [rpm]	$\mathbf{V}_{LL}$ [Vrms]	$\mathbf{I}_g$ [A]	$\mathbf{PF}_g$	$\mathbf{P}_g$ [W]	$\mathbf{I}_{DC}$ [A]	$\mathbf{V}_{DC}$ [V]	$\mathbf{P}_{DC}$ [W]	
1462,00	157,70	5,73	0,97	1.520,0	195,67	7,75	1516,46	1,45
1446,67	155,60	5,63	0,97	1.470,0	188,97	7,72	1458,76	1,41
1364,67	144,53	5,67	0,97	1.380,0	179,43	7,59	1361,18	1,32
1272,00	137,40	5,60	0,97	1.280,0	167,03	7,57	1265,00	1,20
1182,00	124,77	5,70	0,97	1.180,0	153,27	7,59	1163,29	1,11
1091,67	112,77	5,80	0,96	1.090,0	137,87	7,75	1068,93	1,02
1005,33	103,80	5,80	0,96	1.000,0	124,77	7,83	976,92	0,93
928,67	97,50	5,60	0,96	910,0	118,60	7,57	897,41	0,86
875,00	97,17	5,10	0,96	830,0	118,40	6,94	821,70	0,79
831,00	97,53	4,70	0,96	760,0	118,30	6,30	745,29	0,72
798,00	97,87	4,20	0,96	680,0	118,03	5,68	670,82	0,66
769,00	97,57	3,80	0,95	600,0	118,20	5,04	596,04	0,59
745,00	97,73	3,23	0,95	540,0	118,50	4,45	527,72	0,52
723,33	97,80	2,80	0,94	450,0	118,17	3,66	432,88	0,45
704,00	97,47	2,30	0,93	360,0	118,40	3,02	357,57	0,37
678,00	96,27	1,80	0,92	280,0	117,93	2,35	277,54	0,30
651,00	94,63	1,40	0,92	200,0	118,63	1,62	191,79	0,20
616,33	92,30	0,70	0,91	100,0	118,43	0,90	106,20	0,11

Table A.3: Grid-connection test with generator 60R110-4S3P-S-HP and Sunny Boy 2100TL.

N [rpm]	$\mathbf{V}_{LL}$ [Vrms]	$\mathbf{I}_g$ [A]	$\mathbf{PF}_g$	$\mathbf{P}_g$ [W]	$\mathbf{I}_{DC}$ [A]	$\mathbf{V}_{DC}$ [V]	$\mathbf{P}_{DC}$ [W]	
1484,00	150,30	6,03	0,97	1.530,0	190,70	7,90	1506,85	1,39
1435,67	150,37	5,83	0,97	1.470,0	181,57	7,90	1434,98	1,34
1343,67	140,77	5,80	0,97	1.370,0	168,87	7,90	1333,48	1,24
1258,67	131,50	5,80	0,97	1.270,0	160,70	7,80	1252,92	1,15
1172,67	122,30	5,73	0,96	1.180,0	149,87	7,69	1152,97	1,06
1090,00	112,83	5,73	0,96	1.090,0	139,53	7,63	1064,64	0,97
1011,67	109,90	5,43	0,96	990,0	129,70	7,50	973,18	0,89
955,00	106,50	5,20	0,96	920,0	128,47	7,02	901,84	0,82
913,33	105,47	4,80	0,96	840,0	129,60	6,37	825,12	0,74
872,33	106,50	4,30	0,96	770,0	128,27	5,86	751,64	0,68
844,00	103,60	4,10	0,96	710,0	127,83	5,33	681,78	0,61
820,33	105,93	3,43	0,95	600,0	129,70	4,50	584,08	0,53
793,67	106,07	3,00	0,94	510,0	129,33	3,93	508,71	0,48
782,00	106,37	2,50	0,93	430,0	130,07	3,31	430,09	0,36
748,67	105,03	2,20	0,93	370,0	126,77	2,96	374,81	0,30
715,33	101,60	1,90	0,93	300,0	127,30	2,52	320,80	0,25
694,00	102,10	1,10	0,93	180,0	131,90	1,17	154,32	0,14
663,00	98,23	0,80	0,92	130,0	128,43	0,74	95,04	0,06

Table A.4: Grid-connection test with generator 60R120-6S2P-S-HP and Sunny Boy 1.5.

N [rpm]	$\mathbf{V}_{LL}$ [Vrms]	$\mathbf{I}_g$ [A]	$\mathbf{PF}_g$	$\mathbf{P}_g$ [W]	$\mathbf{I}_{DC}$ [A]	$\mathbf{V}_{DC}$ [V]	$\mathbf{P}_{DC}$ [W]	
1460,67	261,77	3,30	0,97	1.450,0	325,36	4,43	1440,28	1,39
1367,67	261,90	3,00	0,96	1.290,0	324,17	3,98	1289,13	1,25
1327,00	258,93	2,80	0,96	1.200,0	323,77	3,72	1204,42	1,18
1197,67	230,33	2,90	0,96	1.130,0	281,82	3,95	1112,24	1,09
1157,33	227,30	2,80	0,96	1.040,0	279,57	3,72	1040,01	1,01
1117,00	227,30	2,60	0,96	960,0	276,68	3,49	966,52	0,94
1063,33	223,53	2,40	0,95	880,0	267,59	3,30	883,05	0,86
884,33	165,97	2,90	0,96	810,0	203,01	3,97	805,26	0,78
787,00	144,70	3,00	0,96	730,0	173,46	4,16	721,61	0,69
723,67	132,43	3,00	0,96	660,0	162,06	4,04	655,28	0,63
661,67	122,00	2,90	0,95	590,0	148,66	3,95	587,22	0,56
580,33	104,13	3,00	0,95	510,0	126,79	4,05	513,91	0,49
556,67	108,50	2,60	0,95	460,0	132,81	3,40	452,00	0,43
515,67	105,40	2,30	0,95	400,0	127,30	3,09	392,93	0,37
469,00	99,30	2,00	0,94	330,0	119,04	2,73	324,98	0,31
420,33	89,83	1,80	0,94	270,0	108,51	2,45	265,85	0,24
343,00	56,03	2,20	0,94	200,0	89,01	2,54	226,09	0,18
227,33	47,73	1,80	0,93	140,0	55,68	2,48	138,09	0,12

Table A.5: Grid-connection test with generator 60R120-6S2P-S-HP and Omniksol.

N [rpm]	$\mathbf{V}_{LL}$ [Vrms]	$\mathbf{I}_g$ [A]	$\mathbf{PF}_g$	$\mathbf{P}_g$ [W]	$\mathbf{I}_{DC}$ [A]	$\mathbf{V}_{DC}$ [V]	$\mathbf{P}_{DC}$ [W]	
1360,67	227,17	3,60	0,96	1.360,0	280,81	4,83	1357,25	1,33
1274,33	217,50	3,50	0,96	1.270,0	267,07	4,72	1260,57	1,21
1196,00	206,77	3,40	0,96	1.180,0	251,08	4,68	1174,20	1,13
1123,00	192,73	3,40	0,96	1.100,0	237,88	4,58	1089,48	1,05
1055,67	189,80	3,30	0,96	1.030,0	226,93	4,50	1021,20	0,98
986,33	174,97	3,30	0,96	950,0	212,90	4,44	944,55	0,91
921,67	161,00	3,30	0,96	880,0	201,31	4,27	858,91	0,84
851,33	147,80	3,30	0,96	800,0	186,76	4,32	806,18	0,78
783,33	143,17	3,10	0,96	740,0	172,97	4,22	730,50	0,71
698,00	134,30	2,90	0,96	650,0	149,16	4,34	647,83	0,63
610,67	104,90	3,40	0,93	570,0	121,87	4,61	561,82	0,56
580,00	101,43	3,10	0,93	510,0	119,28	4,23	504,55	0,50
531,33	97,80	2,80	0,95	450,0	118,25	3,77	445,40	0,45
495,33	97,50	2,40	0,95	390,0	118,23	3,26	385,82	0,40
468,67	97,40	2,07	0,94	330,0	118,19	2,70	319,10	0,34
446,67	97,80	1,60	0,93	260,0	118,15	2,23	263,86	0,28
421,67	96,20	1,20	0,92	190,0	118,03	1,61	190,42	0,36
394,67	94,00	0,77	0,91	110,0	118,37	1,00	118,76	0,12

Table A.6: Grid-connection test with generator 60R120-6S2P-S-HP and Sunny Boy 2100TL.

N [rpm]	$\mathbf{V}_{LL}$ [Vrms]	$\mathbf{I}_g$ [A]	$\mathbf{PF}_g$	$\mathbf{P}_g$ [W]	$\mathbf{I}_{DC}$ [A]	$\mathbf{V}_{DC}$ [V]	$\mathbf{P}_{DC}$ [W]	
1332,00	226,37	3,60	0,96	1.350,0	278,33	4,81	1338,75	1,25
1261,67	220,63	3,40	0,96	1.260,0	278,29	4,47	1244,88	1,16
1185,67	207,90	3,40	0,96	1.180,0	257,30	4,53	1166,41	1,08
1116,67	198,33	3,30	0,96	1.090,0	245,67	4,45	1092,40	1,00
1053,33	188,90	3,20	0,96	1.020,0	232,02	4,34	1006,98	0,93
989,00	180,13	3,13	0,96	940,0	219,39	4,25	932,41	0,86
930,00	167,70	3,10	0,96	870,0	211,97	4,08	865,18	0,79
855,00	151,23	3,17	0,96	790,0	191,04	4,14	791,53	0,72
779,67	136,60	3,20	0,96	720,0	172,56	4,16	718,41	0,65
719,67	137,30	2,90	0,95	660,0	161,67	3,99	645,60	0,59
667,00	123,77	2,90	0,95	580,0	154,32	3,74	576,63	0,52
602,33	117,13	2,70	0,95	520,0	140,79	3,62	510,13	0,46
548,00	107,60	2,60	0,95	460,0	129,61	3,46	448,88	0,40
515,00	106,63	2,20	0,95	380,0	129,46	2,66	343,92	0,34
488,33	109,40	1,80	0,93	320,0	126,99	2,54	322,55	0,28
471,00	106,47	1,50	0,92	250,0	127,42	1,90	242,10	0,21
444,00	101,97	1,10	0,92	180,0	127,47	1,44	183,56	0,15
425,00	99,23	0,70	0,91	110,0	130,86	0,78	101,63	0,07

Table A.7: Grid-connection test with generator 60R90-6S2P-S-HP and Sunny Boy 1.5.

N [rpm]	$\mathbf{V}_{LL}$ [Vrms]	$\mathbf{I}_g$ [A]	$\mathbf{PF}_g$	$\mathbf{P}_g$ [W]	$\mathbf{I}_{DC}$ [A]	$\mathbf{V}_{DC}$ [V]	$\mathbf{P}_{DC}$ [W]	
1465,67	163,07	4,90	0,96	1.340,0	200,73	6,34	1273,32	1,21
1459,33	160,03	5,00	0,96	1.330,0	197,50	6,40	1264,66	1,20
1373,67	154,07	4,90	0,96	1.250,0	186,27	6,37	1185,90	1,13
1281,67	148,03	4,70	0,96	1.170,0	184,93	5,96	1101,59	1,05
1190,00	136,87	4,70	0,96	1.070,0	163,97	6,22	1019,87	0,96
1104,33	129,90	4,60	0,96	1.000,0	154,67	6,08	940,89	0,89
1024,67	122,20	4,50	0,96	910,0	146,70	5,93	869,93	0,81
953,33	113,13	4,40	0,96	830,0	135,27	5,76	779,14	0,74
871,00	104,00	4,40	0,96	750,0	127,63	5,64	719,85	0,67
806,00	97,97	4,20	0,96	680,0	121,47	5,38	653,09	0,61
714,00	86,50	4,23	0,95	610,0	104,70	5,45	570,96	0,53
658,67	86,43	3,80	0,95	540,0	102,23	4,99	510,49	0,48
583,67	71,17	4,00	0,95	470,0	90,67	4,90	443,96	0,41
527,00	71,10	3,43	0,95	400,0	83,07	4,63	384,88	0,35
490,33	66,83	3,00	0,94	330,0	82,93	3,86	319,85	0,29
377,67	47,00	3,50	0,95	270,0	59,50	4,27	253,87	0,23
369,00	52,90	2,40	0,93	210,0	65,73	2,99	196,76	0,17
294,00	45,07	2,00	0,93	140,0	54,53	2,45	133,61	0,12

Table A.8: Grid-connection test with generator 60R90-6S2P-S-HP and Omniksol.

N [rpm]	$\mathbf{V}_{LL}$ [Vrms]	$\mathbf{I}_g$ [A]	$\mathbf{PF}_g$	$\mathbf{P}_g$ [W]	$\mathbf{I}_{DC}$ [A]	$\mathbf{V}_{DC}$ [V]	$\mathbf{P}_{DC}$ [W]	
1465,33	177,05	4,50	0,96	1.323,3	217,37	6,16	1339,70	1,28
1398,00	169,07	4,50	0,96	1.260,0	204,10	6,14	1252,49	1,19
1309,67	160,07	4,40	0,96	1.166,7	195,17	6,08	1185,96	1,08
1219,67	147,00	4,47	0,96	1.086,7	179,37	6,09	1092,94	1,03
1176,67	151,20	4,07	0,96	1.016,7	185,13	5,49	1015,76	0,97
1083,00	137,17	4,13	0,95	936,7	167,37	5,61	939,48	0,89
987,33	120,23	4,30	0,95	856,7	147,20	5,88	866,03	0,82
919,33	115,00	4,20	0,95	790,0	138,00	5,70	787,06	0,75
820,33	97,73	4,37	0,95	703,3	117,97	5,84	688,53	0,65
770,00	97,23	4,00	0,95	640,0	118,03	5,43	640,92	0,62
731,67	97,20	3,63	0,95	580,0	117,50	4,94	580,45	0,56
698,00	97,37	3,27	0,94	516,7	117,93	4,37	515,37	0,51
669,00	97,17	2,90	0,94	450,0	118,07	3,82	450,62	0,45
644,00	97,17	2,50	0,93	386,7	117,50	3,25	381,88	0,39
616,00	96,43	2,03	0,93	313,3	117,87	2,63	309,99	0,32
588,00	95,43	1,60	0,93	243,3	117,63	2,04	239,97	0,26
557,33	93,80	1,10	0,92	170,0	118,00	1,37	161,66	0,16
532,00	91,90	0,60	0,91	80,0	118,10	0,69	81,10	0,10

Table A.9: Grid-connection test with generator 60R90-6S2P-S-HP and Sunny Boy 2100TL.

N [rpm]	$\mathbf{V}_{LL}$ [Vrms]	$\mathbf{I}_g$ [A]	$\mathbf{PF}_g$	$\mathbf{P}_g$ [W]	$\mathbf{I}_{DC}$ [A]	$\mathbf{V}_{DC}$ [V]	$\mathbf{P}_{DC}$ [W]	
1466,00	168,90	4,77	0,96	1.340,0	206,43	6,26	1291,58	1,17
1465,00	165,83	4,80	0,96	1.340,0	205,37	6,28	1289,70	1,17
1406,33	160,00	4,80	0,96	1.280,0	199,83	6,18	1234,97	1,12
1301,00	153,47	4,60	0,96	1.180,0	185,67	6,13	1137,52	1,03
1218,00	147,70	4,50	0,96	1.100,0	176,53	5,97	1054,49	0,95
1127,00	129,07	4,70	0,96	1.000,0	164,87	5,88	969,97	0,80
1047,67	122,50	4,50	0,96	920,0	154,03	5,81	895,45	0,80
976,67	119,47	4,30	0,96	850,0	147,87	5,50	812,77	0,73
886,33	106,97	4,30	0,96	760,0	131,27	5,61	736,41	0,65
830,00	107,60	4,00	0,95	710,0	128,63	5,20	668,89	0,59
787,67	106,23	3,60	0,95	630,0	128,10	4,67	598,65	0,53
755,00	106,13	3,20	0,95	560,0	129,17	4,10	529,58	0,46
723,00	106,07	2,80	0,94	490,0	125,50	3,72	467,28	0,40
692,67	107,80	2,30	0,93	400,0	125,83	3,13	393,86	0,33
681,00	102,47	2,10	0,93	350,0	129,53	2,44	316,06	0,26
635,67	103,90	1,60	0,93	260,0	125,77	1,94	243,57	0,19
597,67	102,60	1,10	0,93	180,0	126,37	1,21	153,32	0,12
578,67	100,30	0,60	0,92	100,0	129,10	0,52	67,13	0,04

Appendix B

Platform Tests Full Data

Table B.1: Lh400 platform test with Omniksol-2k-TL2

F [Hz]	**Q** [l/s]	**Head** [m]	$\mathbf{V}_{DC}$ [V]	$\mathbf{I}_{DC}$ [A]	$\mathbf{P}_{DC}$ [W]	$\mathbf{P}_{AC}$ [kW]
60,0	50,04	4,4	177,9	7,18	1276,2	1,22
57,5	46,88	4,4	159,2	6,93	1102,9	1,08
55,0	44,58	4,4	121,1	7,56	915,5	0,90
52,5	41,41	4,4	123,6	6,16	761,8	0,74
50,0	38,33	4,4	144,0	3,72	535,0	0,55
47,5	35,40	4,4	122,4	3,69	451,9	0,45
45,0	31,83	4,4	121,8	2,42	295,1	0,32
42,5	19,88	4,4	117,8	1,56	183,6	0,17
40,0	7,61	4,4	117,8	0,71	83,6	0,09

Table B.2: Lh400 platform test with Sunny Boy 2100TL

F [Hz]	**Q** [l/s]	**Head** [m]	$\mathbf{V}_{DC}$ [V]	$\mathbf{I}_{DC}$ [A]	$\mathbf{P}_{DC}$ [W]	$\mathbf{P}_{AC}$ [kW]
60,0	50,36	4,4	200,1	5,83	1165,78	1,06
57,5	47,27	4,4	202,0	4,83	976,07	0,89
55,0	44,58	4,4	206,7	3,49	721,54	0,56
52,5	41,57	4,4	185,5	3,22	597,78	0,49
50,0	38,48	4,4	178,8	2,44	435,90	0,34
47,5	35,00	4,4	162,6	2,11	343,41	0,30
45,0	32,07	4,4	148,1	1,61	238,21	0,23
42,5	19,96	4,4	133,5	1,11	148,02	0,12
40,0	10,93	4,4	136,5	0,20	26,87	0,03

Table B.3: PLT350 HP platform tests with Sunny Boy 1.5

F [Hz]	**P** [bar]	$\mathbf{V}_{DC}$ [V]	$\mathbf{I}_{DC}$ [A]	$\mathbf{P}_{DC}$ [W]	$\mathbf{P}_{AC}$ [kW]
45,0	9,52	337,9	4,64	1567,70	1,53
42,5	8,88	298,6	4,84	1446,22	1,40
40,0	8,28	291,4	4,30	1253,02	1,22
37,5	7,70	281,4	3,79	1065,69	1,03
35,0	7,14	273,7	3,16	863,87	0,84
32,5	6,64	262,6	2,59	680,13	0,66
30,0	6,20	177,0	3,23	571,60	0,54
27,5	5,76	163,8	2,59	423,70	0,41
25,0	5,36	157,5	1,97	310,28	0,29
22,5	5,02	144,1	1,50	215,62	0,20
20,0	4,68	134,0	1,03	138,43	0,12
17,5	4,42	123,3	0,65	80,15	0,07

Table B.4: PLT350 HP platform tests with Omniksol-2k-TL2

F [Hz]	**P** [bar]	$\mathbf{V}_{DC}$ [V]	$\mathbf{I}_{DC}$ [A]	$\mathbf{P}_{DC}$ [W]	$\mathbf{P}_{AC}$ [kW]
45,0	9,50	328,7	4,84	1590,91	1,53
42,5	8,86	298,2	4,8	1432,2	1,39
40,0	8,26	275,9	4,6	1261,8	1,20
37,5	7,68	242,5	4,5	1100,8	1,04
35,0	7,12	221,5	4,2	926,7	0,88
32,5	6,66	192,4	3,9	744,5	0,72
30,0	6,20	168,2	3,4	575,2	0,56
27,5	5,76	135,0	3,1	414,3	0,42
25,0	5,34	121,3	2,5	297,5	0,31
22,5	5,00	117,6	1,8	209,4	0,22
20,0	4,68	139,4	1,0	133,8	0,14
17,5	4,40	119,1	0,7	81,8	0,09

Table B.5: PLT350 HP platform tests with Sunny Boy 2100TL

F [Hz]	**P** [bar]	$\mathbf{V}_{DC}$ [V]	$\mathbf{I}_{DC}$ [A]	$\mathbf{P}_{DC}$ [W]	$\mathbf{P}_{AC}$ [kW]
45,0	9,52	328,8	4,86	1599,06	1,46
42,5	8,88	301,8	4,74	1431,54	1,31
40,0	8,26	249,4	4,44	1107,48	1,15
37,5	7,68	244,6	4,47	1094,03	1,00
35,0	7,16	201,8	4,61	929,78	0,84
32,5	6,66	201,3	3,69	742,67	0,67
30,0	6,18	195,2	2,93	571,84	0,51
27,5	5,78	192,4	2,23	429,13	0,38
25,0	5,40	163,5	1,93	315,01	0,27
22,5	5,00	152,7	1,39	212,21	0,18
20,0	4,70	128,0	1,11	142,08	0,11
17,5	4,42	128,7	0,63	80,65	0,05

Table B.6: TRG350 HP platform tests with Sunny Boy 1.5

F [Hz]	**P** [bar]	$\mathbf{V}_{DC}$ [V]	$\mathbf{I}_{DC}$ [A]	$\mathbf{P}_{DC}$ [W]	$\mathbf{P}_{AC}$ [kW]
45,0	7,66	338,1	4,63	1566,38	1,52
42,5	7,24	268,6	5,29	1421,79	1,38
40,0	6,80	260,2	4,42	1149,94	1,14
37,5	6,42	247,0	3,82	943,54	0,91
35,0	6,04	275,5	2,76	759,55	0,74
32,5	5,68	269,6	2,20	592,15	0,57
30,0	5,38	254,9	1,76	449,47	0,43
27,5	5,08	188,9	1,77	333,72	0,30
25,0	4,82	196,9	1,17	229,72	0,21
22,5	4,56	189,3	0,77	146,39	0,13
20,0	4,34	176,7	0,47	82,44	0,07
17,5	4,42	128,7	0,63	80,65	0,05

Table B.7: TRG350 HP platform tests with Omniksol-2k-TL2

F [Hz]	**P** [bar]	$\mathbf{V}_{DC}$ [V]	$\mathbf{I}_{DC}$ [A]	$\mathbf{P}_{DC}$ [W]	$\mathbf{P}_{AC}$ [kW]
45,0	7,68	239,8	6,41	1537,92	1,47
42,5	7,22	203,2	6,1	1242,9	1,16
40,0	6,78	191,1	5,2	993,1	0,94
37,5	6,40	137,8	5,1	697,9	0,67
35,0	6,02	123,2	4,2	522,6	0,51
32,5	5,68	121,9	3,6	437,7	0,43
30,0	5,36	120,4	2,9	347,2	0,36
27,5	5,04	119,2	2,3	270,2	0,28
25,0	4,78	117,0	1,6	189,2	0,24
22,5	4,54	117,7	1,2	146,7	0,14
20,0	4,34	118,4	0,8	98,3	0,10
17,5	4,42	128,7	0,63	80,65	0,05

Table B.8: TRG350 HP platform tests with Sunny Boy 2100TL

F [Hz]	**P** [bar]	$\mathbf{V}_{DC}$ [V]	$\mathbf{I}_{DC}$ [A]	$\mathbf{P}_{DC}$ [W]	$\mathbf{P}_{AC}$ [kW]
45,0	7,64	320,6	3,78	1213,06	1,12
42,5	7,20	304,1	3,37	1025,83	0,93
40,0	6,78	275,9	3,38	931,51	0,85
37,5	6,40	247,0	3,25	803,57	0,75
35,0	6,02	217,8	3,27	712,93	0,62
32,5	5,68	187,9	3,07	576,75	0,52
30,0	5,36	165,9	2,74	455,21	0,40
27,5	5,08	150,2	2,22	333,44	0,29
25,0	4,78	134,8	1,75	235,84	0,20
22,5	4,54	131,8	1,25	164,75	0,13
20,0	4,32	129,3	0,79	102,12	0,07
17,5	4,42	128,7	0,63	80,65	0,05